Study on Early Hydration Reactions of Cement Clinker using Isothermal Calorimetry

– Influence of C_3A content, SO_3 content, Blaine Number and Mixing Type

Kristina von Mentzer | Building Materials | LTH | Lund University

Study on Early Hydration Reactions of Cement Clinker using Isothermal Calorimetry

- Influence of C_3A Content, SO_3 Content, Blaine Number and Mixing Type

Kristina von Mentzer

LUND
UNIVERSITY

Master Thesis, Report TVBM-5135, Division of Building Materials, Faculty of Engineering, Lund University, Lund, 2024

Title:
Study on the early hydration reactions of cement clinker using isothermal calorimetry – influence of C_3A content, SO_3 content, Blaine number and mixing type

Author: Kristina von Mentzer

Report TVBM-5135
ISRN LUTVDG/TVBM-24/5135-SE

Number of pages: 63
Illustrations: 24

Keywords
Isothermal calorimetry, Cement production, Cement clinker, Cement hydration

---

Byggnadsmaterial
Lunds tekniska högskola
Lunds universitet
Box 118
221 00 Lund

www.byggnadsmaterial.lth.se

Division of Building Materials
Faculty of Engineering
Lund University
P.O. Box 118
SE-221 00 Lund
Sweden
www.byggnadsmaterial.lth.se/english

Sammanfattning

Cement är ett av världens mest använda material och agerar som bindemedel i betong och murbruk. Portlandcement, som är den mest förekommande typen av cement, produceras årligen i en kvantitet av fyra miljarder ton. Cementproduktionen står för ca 7 % av de globala koldioxidutsläppen och det finns ett stort intresse i att hitta alternativa vägar och optimeringsmöjligheter, för att minimera klimatpåverkan av detta så användbara material.

En nyckel för att lyckas med de förändringar som cementtillverkare står inför, är en välutvecklad och träffsäker processkontroll, där isoterm kalorimetri har visat sig användbar för att kunna analysera materialens reaktivitet. Denna är, i sin tur, kopplad till cementens hållfasthet. Produktionen av cement sker i flera steg och själva hjärtat i processen är en roterande ugn, där råmjölet bränns och omvandlas till cementklinker. Klinkern mals sedan med kalciumsulfat (gips) och eventuellt andra kompletterande material, för att skapa den slutliga produkten – cement.

Isoterm kalorimetri används för att mäta den värmeutveckling som sker till följd av olika kemiska processer. I fallet med cement, mäter man den värme som utvecklas, när cementen blandas med vatten och hydratiserar. Det är då viktigt att få en bra omblandning, så att alla delar av provet blir vått, och det finns två grundläggande sätt att uppnå detta på – man kan blanda in-situ eller ex-situ. Det förstnämnda utförs när provet redan befinner sig i kalorimetern och man kan då följa de kemiska reaktionerna direkt från blandningsögonblicket. Ex-situ-blandning sker i stället externt innan provet placeras i kalorimetern. En fördel med den typen av omblandning är att den kan göras kraftigare än in-situ-blandningen.

Målet med detta examensarbete var att studera hydratation av cementklinker med hjälp av isoterm kalorimetri. För detta användes tre olika klinkertyper med olika halter av trikalciumaluminat, betecknat C_3A. Dessa klinkrar hade också malts till tre olika finhetsgrader, så att det totalt fanns nio skilda klinkermjöl. Mätningarna utfördes både manuellt med in-situ-blandning samt automatiserat med ex-situ-blandning i den helt automatiserade isoterma kalorimetern polabCal vid thyssenkrupp Polysius i Neubeckum i Tyskland. Skillnaderna i resultaten mellan de olika blandningstyperna studerades, liksom möjligheterna att blanda klinkerprover utan tillsatt sulfat. De tidiga kalorimetriska resultaten undersöktes och analyserades utifrån möjliga kopplingar till föreliggande kemiska processer. Slutligen analyserades potentiella samband mellan tidiga reaktioner och den så kallade huvudreaktionen, som ofta startar några timmar efter vätningen av provet.

Ex-situ-blandaren och de automatiserade mätningarna genererade betydligt jämnare och mer repeterbara resultat avseende blandningskvalitet och värmeutveckling än de manuellt genomförda experimenten, oberoende av förekomsten av sulfat – emellertid på bekostnad av förlorad tidig kinetik och reaktionsvärme. Ett högre C_3A-innehåll kunde tydligt kopplas till en snabbare initial reaktion med en högre tidig hydratationstopp och en totalt sett större värmeutveckling. För samtliga klinkersorter kunde en stor spridning bland kurvorna från de tidigare hydratationsreaktionerna relateras till stora variationer för huvudreaktionen. Hos de mer finfördelade klinkerproverna uppvisades högre tidiga

värmetoppar och huvudreaktionen påbörjades tidigare än hos de mer grovmalda proverna.

Abstract

Cement is one of the world's most used materials and acts as a binder in concrete and mortar. Portland cement, which is the most common type of cement, is produced annually in a quantity of four billion metric tons. Cement production accounts for approximately 7 % of the global carbon dioxide emissions and there is a great interest in finding alternative routes and optimization possibilities, to minimize the climate impact of this otherwise very useful material.

A key to succeeding with the changes faced by cement manufacturers, is well-developed and accurate process control, where isothermal calorimetry has proven useful for analyzing the reactivity of the materials. This is, in turn, linked to the compressive strength of the cement. Cement production includes several steps, and the very heart of the process is a rotary kiln, in which the raw meal is burned and turned into cement clinker. This clinker is then ground with calcium sulfate (gypsum) and possibly other supplementary materials, to create the final product – cement.

Isothermal calorimetry can measure the heat development that occurs as a result of various chemical processes. In the case of cement, one measures the heat developed when cement is mixed with water and hydrates. It is then important to get a good mixing, so that all parts of the sample become wet, and there are basically two ways to achieve this – either through in-situ or ex-situ mixing. The former is carried out when the sample is already in the calorimeter, and you can then follow the chemical reactions directly from the moment of mixing. Ex-situ mixing, on the other hand, takes place externally before the sample is placed in the calorimeter. An advantage of this type of mixing is that it can be made stronger than the in-situ mixing.

The objective of this thesis was to study the hydration of cement clinker using isothermal calorimetry. For this, three different clinker types with different contents of tricalcium aluminate, designated C_3A, were used. Theses clinkers had also been ground to three different degrees of fineness, so that there was a total of nine different clinker powders. The measurements were performed both manually with in-situ mixing, and automatically with ex-situ mixing in the fully automated isothermal calorimeter polabCal at thyssenkrupp Polysius in Neubeckum, Germany. The differences in the results between the different mixing types were studied, as well as the possibility of mixing clinker samples without added sulfate. The early calorimetric results were examined and analyzed based on possible connections to chemical processes taking place. Finally, connections between the early reactions and the main hydration, often starting a few hours after the wetting of the sample, were examined.

The ex-situ mixer and the automated measurements generated significantly more consistent and repeatable results regarding mixing quality and heat development than the manually conducted experiments, regardless of the presence of sulfate – however, at the expense of lost early kinetics and heat of reaction. A higher C_3A content could clearly be

linked to a faster initial reaction with a higher early hydration peak and an over greater heat release. For all clinker types, a large spread among the early hydration curves could be related to large variations in the curves of the main reaction. The finer ground clinker samples displayed higher early hydration peaks and their main reactions also started sooner than the ones of the more coarsely ground samples.

This project for the degree of Master of Science in Chemical Engineering was carried out at the Division of Building Materials, Department of Building and Environmental Technology, at Lund University.

At the division, Lars Wadsö was main and Edita Garskaite co-supervisor. Paul Sandberg (Cemvision) was industrial supervisor together with Michael Enders (thyssenkrupp Polysius).

Examiner at the Division of Building Materials was Magnus Åhs.

The project was made in cooperation with thyssenkrupp Polysius in Neubeckum, Germany.

Acknowledgements

I would really like to express my gratitude towards my supervisors for all the support throughout this project. Apart from all the rewarding conversations and interesting discussions on everything from civil engineering to sustainability issues, I received plenty of valuable feedback on my work and professional help to navigate through the jungle of cement chemistry. This, undoubtedly, helped me to keep my focus and widened my understanding of and interest for this highly relevant field.

The trip to Neubeckum, Germany, which included a cement plant visit, advanced automated calorimetric measurements, and a valuable exchange of questions and knowledge on the topic, was great for widening my perspective even more and for putting my work in a wider context.

I would also like to express special gratitude to Lars Wadsö for providing me with all the software evaluation tools, which have been central to my data analyses.

Table of Contents

Vocabulary, Processes and Nomenclature

Materials

AFm	Acronym for calcium aluminate ferrite hydrate with mono sulfate (often referred to as “monosulfate”). Important cement hydration product.
AFt	Acronym for calcium aluminate ferrite hydrate with tri sulfate (often referred to as “trisulfate” or the mineral Ettringite)
Aggregate	Sand and rocks forming the major part of concrete.
Alite	Tricalcium silicate (Ca_3SiO_5, ‘C_3S’) with impurities. Usually 50–70 % of PC.
Aluminate	Tricalcium aluminate ($Ca_3Al_2O_6$, ‘C_3A’) with impurities. Highly reactive with water. Important for setting. Usually 5–10 % of PC.
Anhydrite	Anhydrous calcium sulfate ($CaSO_4$ or $C\bar{S}$).
Belite	Dicalcium silicate (Ca_2SiO_4, ‘C_2S’) with impurities. Usually 15–30 % of PC.
Calcite	$CaCO_3$
Calcium Silicate Hydrate	C–S–H. One of the main cement hydration products. Variable stoichiometry.
Calcium Hydroxide	Portlandite ($Ca(OH)_2$, ‘CH’). One of the main cement hydration products.
Cement (Portland)	The most common binder in concrete.
Cement Clinker	Nodulized unground product from the kiln, < 30 mm, that is later ground with calcium sulfate and optional supplementary materials to make cement.
Cement Paste	A paste is a properly proportioned water-cement mixture, in which setting and hardening can take place. The hardened material is also included in this expression.
Concrete	A mixture of fine and coarse aggregates and cement.
Ettringite	$C_3A \cdot 3CaSO_4 \cdot 32H_2O$. Mainly formed early in cement hydration.
Ferrite	Tetracalcium aluminoferrite (C_4AF) with impurities (varying proportions of C, A and F). Gives cement its grey color. 5–15 % of PC.
Gypsum	Calcium sulfate dihydrate ($CaSO_4 \cdot 2H_2O$ or $C\bar{S}_2H$). Added to the clinker in the mill. Acts as setting regulator.

Lime	Calcium oxide (CaO). Unreacted lime in cement is called 'free lime'.
Mortar	A mixture of fine aggregates and cement.
PC	Acronym for *Portland Cement*.
Periclase	Magnesium oxide, periclase. Found in small amounts in PC.
Silica	Silicon dioxide, SiO_2. In nature it often occurs in the form of quartz, which is the main component in sand.
Slag	Blastfurnace slag – a by-product of iron production – can be used to partly replace cement in concrete.
Quartz	A natural mineral consisting mainly of crystalline silica but also impurities.

Chemical processes

Calciner	Additional burner in the preheater tower.
Calcination	Process of removing water or carbon dioxide from a material. Mostly associated with removal of carbon dioxide from limestone.
Clinkering	Nodule formation from the raw meal. Free lime and C_2S combine to form C_3S.
False setting	False setting is stiffening due to the formation of gypsum crystals during hydration as a result of an excessive amount of soluble sulfate in the cement pore fluid. Redissolving of the crystals and, hence, mixing through this type of setting is possible in some cases.
Flash setting	Flash setting denotes stiffening due to the quick reaction of C_3A to form calcium aluminate hydrates because of a lack of soluble sulfate in the cement pore fluid to retard the otherwise very rapid aluminate hydration. As the calcium aluminate hydrate crystals do not easily redissolve, it is not possible to mix through this type of setting.
Hydration	Reactions with water, for example when C_3S reacts with water to form C–S–H and CH, or when C_3A reacts with water to form calcium aluminate hydrates.
Setting	Refers to the initial stiffening of the cement paste, which has not given any considerable compressive strength development.

Cement chemist's nomenclature

In cement chemistry, chemical compounds are often denoted in terms of oxides. Some of the most common abbreviations are listed here.

$C = CaO$	$S = SiO_2$	$A = Al_2O_3$	$F = Fe_2O_3$	$M = MgO$
$K = K_2O$	$\bar{S} = SO_3$	$N = Na_2O$	$H = H_2O$	$\bar{C} = CO_2$

Quality parameters

Lime Saturation Factor (LSF) — Molar quotient of free lime and the three major oxides. For clinkers

$$LSF = \frac{CaO}{2.8SiO_2 + 1.2Al_2O_3 + 0.65Fe_2O_3}.$$

Silica Ratio (SR) — Molar quotient of silica oxides, and alumina and iron oxides in the clinker:

$$SR = \frac{SiO_2}{Al_2O_3 + Fe_2O_3}.$$

Alumina Ratio (AR, A/F) — Molar ratio between C_3A and C_4AF in the clinker:

$$AR = \frac{Al_2O_3}{Fe_2O_3}.$$

1. Introduction

Inorganic cements are a group of extremely common ceramic materials, also known as binders. When mixed with water they react with water, hydrate, to form a paste, that can be shaped as desired before it sets and solidifies [1]. The setting of the material can be described as an initial stiffening, usually occurring within the first few hours, while the hardening process can go on for many years, so the material actually gets stronger with time [2]. As the hardening can take place at low, ambient temperatures, cementitious materials are very practical to use and it is no wonder that Portland cement – the most commonly produced type of cement [1] – is used in huge quantities worldwide in general construction [3].

Portland cement was first patented in 1824 by Joseph Aspdin and named this way, as the cement resembled a natural stone from the Isle of Portland on the southwest coast of England [4]. This type of cement has, accordingly, been in use for about 200 years. However, cementitious materials as such are not new and, in fact, they have played a crucial role in ancient history. In Egypt calcined gypsum was used as a binder, while the Romans and Greeks would heat limestone to make lime and then add sand or stones to produce mortar or concrete, respectively [5]. The Romans also invented a so-called hydraulic cement (later known as 'pozzolanic') by mixing lime with volcanic ash. This type of cement hardens through a chemical reaction with water and since it can set also under water, it was well suited for the construction of harbors.

Up until this day, continuous improvements and adjustments have been made to tailor the various properties required for different kinds of construction. Consequently, different binders exhibit different properties regarding, for example, color, setting time, and final strength. For convenience and clarity, throughout this report, the term 'cement' will, however, be used to refer to Portland cement, unless otherwise specified.

When producing cement, the raw materials limestone and clay are pulverized and blended. This mix is then heated in a rotary kiln up to a temperature of about 1450 °C to enable the desired high temperature clinkering reactions to occur, including the formation of the principal cement minerals C_3S and C_2S from the raw materials prepared with the correct chemical composition. Once formed, the clinker has to cool quite rapidly to prevent decomposition of C_3S. The C_3A and C_4AF phases are important as they form a liquid phase that facilitates efficient formation of C_3S and C_2S. The resulting cement clinker is ground together with a smaller amount of gypsum, that will retard the otherwise very rapidly reacting C_3A phase during the wetting of the cement in later use.

After production, cement is stored as a dry powder but, once hydrated (i.e., mixed with water), it acts like an adhesive, binding different aggregates. Adding sand to the cement paste creates mortar and concrete is made by blending cement with sand and crushed stones [4]. With a worldwide use of three metric tons per person and year concrete is in fact – after water – the second most consumed product on the globe and cement usually makes up 10–15 vol-% of it [6]. In practice, this means that one cubic meter of concrete, weighing approximately 2.2 metric tons, contains about 300 kg of cement.

Every year over four billion metric tons of Portland cement are manufactured [7] and since each metric ton of cement releases nearly 900 kg of carbon dioxide, CO_2, [8] the usage of

Portland cements in the building industry is undoubtedly a major contributor to greenhouse gas emissions. About 7 % of the global CO_2 emissions stem from cement production and, on an industrial scale, the cement industry is the world's third-largest energy consumer [9]. At the same time, as the global population keeps rising along with the demands on infrastructure development, cement production is also expected to increase further within the coming years, for example in Africa and India, where the capacity of cement production most likely will grow as part of the societal development and infrastructure improvement (8).

The expected future expansion of cement production might seem to run counter to all the efforts made to limit CO_2 emissions and global warming, and one can certainly question if this is the right way to go – are there no reasonable alternatives to cement and concrete? Well, you could probably answer both yes and no to this question. On the one hand, biobased building materials can, for example, partly replace concrete in buildings. On the other hand, if we want to keep a similar infrastructural standard and maintain harbors, bridges and railways, while enabling more countries to follow in the same footsteps, binders in general, and cement in particular, will have a given role in the future as well.

Nevertheless, the awareness of the climate impact of cement is high and the issue is addressed in different ways across the globe. In their *Technology Roadmap – Low-Carbon Transition in the Cement Industry* from 2009, the International Energy Agency (IEA) and the Cement Sustainability Initiative (CSI) highlight some measures as the most decisive for sustainable development in cement manufacturing. Typically, 60–70 % of the total process-generated CO_2 emissions originate from limestone decomposition and the last 30–40 % are being released in the fuel combustion required to heat the kiln (8). Therefore, according to IEA and CSI, focus should be on reducing the proportion of clinker in the cement and limiting the discharge of CO_2 in the production. The former can be achieved by partly substituting the clinker with, for example, slag products and the latter by shifting to low-carbon energy sources and/or using carbon capture and storage (CCS) as an integrated part of production (8).

When performing this inevitable transformation of the cement industry, it is however crucial to continuously follow up on the cement quality to ensure a high-quality product and, in the end, safe and durable building constructions. There are many laws and standards regarding this and even if the legal requirements on strength and durability of course need to be met, standards may have to be adjusted to suit the new binders that are being developed.

Both process and quality control are central parts of cement manufacturing. Unfortunately, the growing use of alternative fuels and raw materials (AFRs) makes quality control more complicated [10]. Often, the reactivity of clinker and cement is reduced, or at least modulated. However, within the clinker production part of a cement plant, the reactivity of the clinker is not assessed; this is only done by strength measurements on mortars after the clinker has been ground to cement, several days after the clinker was produced. This makes it hard, if not impossible, to use the analysis of reactivity to control production on an ongoing basis. Nonetheless, this should be the goal, as consistent and predictable production, and ultimately product quality, is the key to optimizing both business economy and the use of cement in building structures.

1.1. Aim

The aim of this master's thesis has been to study the early hydration reactions of cement clinker – that is, reactions taking place during the first approximately 20 min of hydration. The purpose has been to better understand the correlations between cement clinker composition and the later properties of the cement or the final mortar and concrete.

This has been done by means of a manual I-Cal Ultra isothermal calorimeter at the Division of Building Materials at Lund University and an automated polabCal instrument (with the same type of calorimeter) at thyssenkrupp Polysius in Neubeckum, Germany. The former is equipped with an internal (in-situ) mixer, while samples in the latter are blended in an external (ex-situ) mixing device, before being placed into the calorimeter.

The main focus of the work has been on the following:

1) Examining differences between the results generated from measurements with in-situ and ex-situ mixing, respectively, and investigating to which extent it is possible to mix clinker samples without further addition of SO_3 – is there a difference regarding this between the in-situ and ex-situ mixing?
2) Understanding, how the early calorimetric results can be interpreted in terms of chemical processes within the sample.
3) Examining the connection between the early hydration reactions and the main reaction.

1.2. Limitations

The project was limited to the nine cement clinker samples provided by thyssenkrupp Polysius.
The automated measurements were limited in terms of the time available to perform them.

2. Cement

Before considering hydration reactions, it makes sense to gain some general understanding of cement composition and how the manufacturing process is designed to tailor exactly this.

The following sections contain a lot of detailed information on cement chemistry and cement production. Unless otherwise stated, the book *Cement Chemistry* by H. F. W. Taylor [3] has been used as reference.

It is also worth noting that cement chemists often use a certain nomenclature, which differs from the universal one. This has been developed to shorten and simplify the notation of all the compounds present in cement chemistry. As an example, according to this system, calcium oxide, CaO, is denoted 'C', while 'S' is the abbreviation of silicon oxide, SiO_2. For further explanation on these abbreviations, see the section *Vocabulary, Processes and Nomenclature*.

Because Portland cement is by far the most common type of cement in the world, this will also be the main focus of this report. It is sometimes also referred to as *Ordinary Portland Cement (OPC)* or just *Ordinary cement (OC)*.

2.1. Portland cement

2.1.1. General composition

Portland cement contains four major phases known as alite, belite, aluminate, and ferrite. Alite ($3CaO \cdot SiO_2$, 'C_3S') is the dominating phase, usually constituting 50-70% of the material. About 15-30 % consists of belite ($2CaO \cdot SiO_2$, 'C_2S'), while aluminate ($3CaO \cdot Al_2O_3$), 'C_3A') and ferrite ($4CaO \cdot Al_2O_3 \cdot Fe_2O_3$, '$C_4AF$') mostly make up approximately 5-10% and 5–15%, respectively [3, 4]. It is when these phases are hydrated, i.e. undergo reactions with water, that the cement transitions from its state as a dry powder to form a hard mass.

C_3A is the phase with the main influence on the setting and early strength development (first few days) of the hydrating cement. C_3S is the most desired cement mineral as it contributes to most of the strength development up to 28 days, which is the typical age used for designing concrete structures, while C_2S impacts the later strength development. The C_4AF and C_3A phases facilitate the cement clinker production at a practically reasonable kiln temperature, as it is part of the liquid phase necessary during the reactions in the cement kiln. An overview of the four main clinker phases and their impact on hydration is presented in Table 1.

Table 1. The four main phases of cement clinker and some of their properties.

Phase	Chemical formula	IUPAC name	Cement chemist notation	Constituted share (%)	Reaction with water	Impacts
Alite	Ca_3SiO_5	Tricalcium silicate	C_3S	50–70	Relatively quick	Strength development during the first 28 days
Belite	Ca_2SiO_4	Dicalcium silicate	C_2S	15–30	Slow	Strength development after 28 days
Aluminate	$Ca_3Al_2O_6$	Tricalcium aluminate	C_3A	5–10	Quick	Setting and very early strength development
Ferrite	Ca_2AlFeO_5	Tetracalcium aluminoferrite	C_4AF	5–15	Variable	Liquid formation during production. Dark color.

All the above phases exhibit different polymorphic modifications, which means that they can occur in various forms, depending on the thermodynamic and kinetic circumstances during formation. The prevalence of substituent ions, such as Na^+, K^+ and Mg^{2+}, further modifies and distorts the phases by promoting the formation of certain structures. As a result, C_3S is mostly present in a monoclinic structure known as M3 and for C_2S, the so-called β polymorph, β-C_2S, is predominant.

On an oxide basis, cement clinker is typically composed of CaO (67%), SiO_2 (22%), Al_2O_3 (5%), Fe_2O_3 (3%) and other components (3%).

2.1.2. International standards

There are two leading standards in the world dealing with different types of Portland cements – ASTM C150 and EN 197. These are the prevailing North American and European Standards, respectively. The British Standard BS 12, which was used for several decades, has been replaced by BS EN197 but still serves as a fundament in some countries.

ASTM C150

The ASTM C150 is provided by the American Society for Testing and Materials and is called 'Standard Specification for Portland Cement' [11]. It includes a description of the ingredients allowed, as well as requirements of a chemical and physical nature – for example, limits regarding the containment of free lime and certain oxides and silicates. The test methods for determination of the relevant properties are also indicated.

According to this standard, Portland cement is divided into eight categories, or 'types': Type I and IA, Type II and IIA, Type III and IIIA, Type IV, and Type V.

- *Type I* covers general purpose cements used when the special properties of other cement types are not required.
- *Type II* cements are for general use and, more specifically, when moderate sulfate resistance or moderate heat of hydration is required.
- *Type III* cements have a high early strength.
- *Type IV* cements have a low heat of hydration.
- *Type V* cements have a high sulfate resistance.

The 'A' occurring in combination with Type I, II and III designates air-entraining cements, which are sometimes preferred. Air entrainment is, namely, an efficient measure to enhance the resistance of concrete to the effects of freezing and thawing [12].

EN 197

The European Standard EN 197 provides definitions and "specifications of 27 distinct common cements, 7 sulfate resisting common cements as well as 3 distinct low early strength blast furnace cements and 2 sulfate resisting low early strength blast furnace cements and their constituents" [13]. The cements are assigned to one of nine strength classes. The definition of every cement includes the proportions of the ingredients constituting the different cements, as well as the chemical, physical, and mechanical requirements. According to this, the 27 common cements can be divided into five main types:

- *CEM I* – Portland cement
- *CEM II* – Portland-composite cement
- *CEM III* – Blastfurnace cement
- *CEM IV* – Pozzolanic cement
- *CEM V* – Composite cement

The standards regarding cement testing methods are given in the European Standard EN 196.

Furthermore, there are different standards regarding concrete, which can be seen as another dimension, that the cement needs to fit into.

One particular example of a compound, whose content needs to be controlled is magnesium oxide, MgO. This is a common minor component in clinker with a remarkable impact on the properties of the both the clinker and the final cement and concrete [14]. When present in a certain amount, it promotes clinker formation in the kiln by enhancing the reactivity and it also has an influence on the phase composition [14] (more about clinker formation can be found in the section *2.2 Portland cement production*). In the final clinker it mainly resides in the form of free MgO – a crystalline phase known as periclase – and, as such, it poses a threat to concrete structures. Periclase can namely cause delayed expansion of the cement as the crystals hydrate and form brucite, $Mg(OH)_2$; the solid volume can then increase by 18% [14]. This expansion of hardened concrete, resulting from slow reaction with water, is a potential threat to building constructions and it is therefore of highest importance to monitor the MgO content. In Portland cement clinker it is limited to a maximum of 5 % [3].

The sulfate content is likewise limited by the specifications given in the standards. It should also be noted that there are two types of sulfate present in cement – one type is already included in the raw material, while the other type is added during the grinding of the clinker. The right sulfate content is crucial for the setting of the material; if there is too little soluble sulfate available during cement hydration, the material risks so-called flash setting. An excessive amount of soluble sulfate, on the other hand, may induce false setting and also volume instability at later ages (so called delayed ettringite expansion) (see *Vocabulary, Processes and Nomenclature* for further explanations on false and flash setting).

2.1.3. Quality assurance and parameters

When it comes to ensuring a good cement clinker quality, several factors need to be considered. Among these are chemical, or compositional, parameters referring to oxide components. Therefore, oxide analyses are conducted on the raw materials and based on this information, one can conclude or, at least, get a hint regarding several properties of the clinker.

The so-called Bogue calculation can be used to quantitatively estimate the final phase composition of the clinker, based on the oxide analysis of the raw material. One should, however, be aware that the model includes certain assumptions and simplifications – for example, only pure phases are considered. Also, in reality, the chemical reactions taking place in the kiln do not all go to completion which means that the result of the calculation shows the potential but not the actual composition. Nevertheless, the Bogue equations can be used when designing the raw mix at the beginning of the production process.

In clinker production, C_3S formation is a key step and most parameters regulating the process therefore focus on supporting this reaction [15]. Here, for example, the raw meal fineness plays a role. There are three chemical parameters, in particular, that are commonly considered within cement chemistry, namely the Lime Saturation Factor (LSF), the Silica Ratio (SR), and the Alumina Ratio (AR). These will now be described in more detail.

Lime Saturation Factor (LSF)

The LSF is defined as the molar quotient of free lime, CaO, and the other three major oxides. For clinkers it is determined according to:

$$\mathrm{LSF} = \frac{\mathrm{CaO}}{2.8\mathrm{SiO_2} + 1.2\mathrm{Al_2O_3} + 0.65\mathrm{Fe_2O_3}}.$$

To calculate the LSF for cement (containing $C\bar{S}_2$), $0.7SO_3$, is subtracted from the amount of CaO.

The LSF regulates the ratio between C_3S and C_2S – a high LSF clinker will contain more C_3S in relation to C_2S and vice versa – and it indicates if an undesirable share of free lime can be presumed. When LSF=1.0, this implies that all free lime will react with C_2S to form C_3S. A value ≥1 suggests that there will be free lime present at equilibrium at the clinkering temperature, and probably it will remain also in the product.

Excess free lime not only leads to higher burn of clinker, grinding difficulties and an increased energy demand, but also to undesirable outcomes of the final cement, such as a decreased reactivity, increased setting time and, in the end, a reduced strength of the cement [16].

In practice, an LSF <1.02 can be accepted but, typically, the values are in the range of 0.92– 0.98.

Silica Ratio (SR)

The SR expresses the molar ratio of silica oxides, and the alumina and iron oxides present in the clinker:

$$\mathrm{SR} = \frac{\mathrm{SiO_2}}{\mathrm{Al_2O_3} + \mathrm{Fe_2O_3}}.$$

The higher the SR, the more calcium silicates are in the clinker. Consequently, there is less C_3A and C_4AF, which impacts the clinkering reactions by lowering the liquid content present at any temperature in the kiln. In other words, the more silica present, the harder it will be to burn the clinker and form the desired phases. More energy, i.e., fuel will also need to be fed into the system. A lower SR, on the other hand, promotes liquid formation, which enhances clinker burnability and lowers fuel consumption.

For normal Portland cements, SR typically has a value of 2.0–3.0.

Alumina Ratio (AR)

The AR (sometimes denoted A/F) determines the ratio between C_3A and C_4AF in the clinker and is defined as:

$$\mathrm{AR} = \frac{\mathrm{Al_2O_3}}{\mathrm{Fe_2O_3}}.$$

The impact of the AR is somewhat more intricate than the ones of the other two parameters. According to Harrisson [17], there are four important outcomes depending on the AR. Firstly, the AR regulates the amount of liquid that can form at lower temperatures in the kiln, with a value of 1.38 giving the most liquid at the lowest temperatures. Secondly, a high AR gives a more viscous liquid, which, in turn, makes it more difficult for the right combinations to occur. Thirdly, at any given LSF, a high AR leads to less C_3S being formed and, fourthly, a low AR causes more C_4AF to be produced, which affects the final color of the clinker and cement – the more C_4AF, the darker the material and, correspondingly, high alumina ratios generate white cements.

The alumina ratio also determines other properties of the cement; darker cements exhibit a higher sulfate resistance and improved durability.

2.1.4. Tests and analyses

The primary aim of cement production is to consistently provide a high-quality product by mixing and grinding certain minerals and transform these into another set of minerals, all while minimizing costs and maximizing efficiency. As outlined earlier, C_3S formation is crucial and, hence, both the amount of C_3S as well as its crystal size and reactivity are essential for clinker quality.

For this part on tests and analyses, the book section *4 - Constitution and Specification of Portland Cement* written by A. M. Harrisson in *Lea's Chemistry of Cement and Concrete (Fifth Edition)* [17] has been used as reference, with a few exceptions that are separately indicated.

There are different analytical methods available for analyzing cement and cement clinker. For this purpose, wet chemical methods have commonly been used. As this, however, requires a laboratory with a good supply of well-trained personnel working around the clock, modern cement plants tend to move increasingly to automated sampling and analyses.

Microscopy

Optical (or light) microscopy is a well-tried and, in many ways, advantageous technique to examine cement clinker. It generates plenty of data and can be used to gain knowledge on both particle shape and particle size distribution (PSD). It also helps in understanding the microstructure of clinker and, hence, allows the study of the changes occurring in the production process. Furthermore, optical microscopy can help in troubleshooting problems within the production process and identifying the areas of manufacturing that should be improved. It is commonly used to keep track of the processes in the kiln.

Scanning electron microscopy (SEM) is another common means used in laboratories to examine clinker compositions. By coupling it with an X-ray analyzer and then letting the electron beam focus on a single crystal, the thereby generated x-rays can be collected and interpreted in form of a chemical analysis. Repeating the procedure on all the different types of crystals provides an average composition of each individual phase. In comparison to the Bogue calculation, this is a more accurate way to determine phase compositions.

XRF and XRD

X-ray fluorescence (XRF) spectrometry is a common, non-destructive way of chemically analyzing samples both qualitatively and quantitatively for their content of various elements. The samples are exposed to a primary X-ray beam, exciting the elements within the sample, and making them emit secondary radiation of element characteristic wavelengths and with intensities mirroring the concentration of the individual elements. These are then converted to oxides to fit into cement chemistry calculations. Clinker is often checked on its content of the four main oxides, mentioned earlier, namely CaO, SiO_2, Al_2O_3, and Fe_2O_3 (or C, S, A and F in the cement chemist's notation).

X-ray diffraction (XRD) is another frequently used technique, measuring the crystal parameters of materials based on electron density, giving rise to a certain diffraction pattern as an X-ray beam is fired through the sample. By comparing the generated diffraction patterns to the ones of already known crystal structures, knowledge can be gained on the different crystal forms and, thus, phases present. In the case of cement clinker, this can provide knowledge about the occurrence of both the main phases C_3S, C_2S, C_3A, and C_4AF, and also free lime and periclase. There is, however, an important difference between free lime detected by XRD and by the traditional wet ethylene glycol method; the latter will namely find also anhydrous as well as hydrated free lime, while XRD addresses only free lime if not otherwise programmed. XRD results will also show lower values in partly hydrated cements.

The use of XRD requires a certain knowledge of the phases analyzed and it can be hard to quantify phases that vary a lot in their composition, like for example C_4AF. C_4AF is one of the phases that turn liquid in the kiln and depending on aspects like cooling rate and oxidation state by the time of crystallization, this gives rise to compositional variations.

Both XRF and XRD are used industrially to analyze the clinker after it leaves the kiln as well as the final cement. For the raw mix, coming out of the raw mill, XRF is often used.

Compressive strength measurements

Compressive strength measurements are a type of examination performed at the very end of the production process in the physical laboratory. It is a common way to quantify cement reactivity, which, nevertheless, is a slow and costly method taking everything from days to weeks [10].

It also comes with a margin of error of 3–5 % [10]. Mathematical analyses are then applied to correlate the physical data with the data provided by the chemical and mineralogical analyses [10].

Cement fineness

The fineness of a cement is an important parameter as this has a direct impact on the hydration kinetics – the smaller the grains, the larger the total surface area of the material and the faster the cement will react when getting in contact with water. The specific surface area (SSA), expressed in cm^2/g or m^2/kg, is oftentimes used to quantify cement fineness. It is commonly determined by means of air permeability methods, where air is

passed through a bed of cement powder. The specific surface area is then calculated from several factors like the cement density, the air flow rate, and the difference in pressure across the bed.

The Blaine method is one of these methods, measuring the time required for a predefined air volume to pass through a bed of ground cement clinker or cement. The obtained Blaine value expresses the specific surface area. Modern ordinary Portland cements typically have a value of 3000–3500 cm^2/g and rapid-hardening Portland cements often have values of 4000–4500 cm^2/g.

Particle size can also be described in terms of particle size distribution (PSD). For particular sizes above 45 μm, sieving is an applicable method, while the full range of size is commonly examined by sedimentation or light diffraction methods. Nonetheless, all the methods carry a certain degree of uncertainty regarding the result interpretation. Agglomeration of particles and the shape of these are examples of factors increasing the complexity of the models.

It can also, in fact, be somewhat problematic to try to link SSA directly to cement reactivity. Different cement phases namely exhibit various degrees of fracture toughness and, accordingly, grindability, which is defined by the energy needed to pulverize a specified amount of material to a certain PSD [18]. As both fine limestone and $C\bar{S}H_2$, included in the cement, are easier milled than the actual clinker, these often contribute to the main part of the SSA without increasing the reactivity. In this case, sieving at 45 μm can be a partial solution as the retained material will mainly be clinker, while the finer particles, of predominantly lime and $C\bar{S}H_2$, will pass through.

The Zeisel method is one of the main methods for determining grindability of brittle and hard materials [19]. The torque of the mill is measured at constant revolution speed and then used together with the angular velocity to calculate the grinding work W (Nm) [19]. The specific energy consumption E_{spec} ($kWht^{-1}$) can then be determined by including the sample mass into the calculation. The results can be used to, among other things, design grinding equipment [19]. It should, however, be noted that grindability is a property related to a system, and not a material; the mechanism of energy transfer to the material largely impacts the grinding result [19]. Furthermore, the collected test values vary with the choice of test parameters like die load, targeted fineness, temperature, and humidity – these are namely not standardized within the industry [19].

2.2. Portland cement production

As explained in the section *2.1.1 General composition*, Portland cement clinker contains four main oxides, and these can be created from various raw materials. There are, however, some essential components required to produce cement – silica (SiO_2, 'S'), calcite ($CaCO_3$, '$C\bar{C}$'), alumina (Al_2O_3, 'A') and iron (III) oxide (Fe_2O_3, 'F') [4].

In practice, cement is typically manufactured by heating the raw meal – a crushed, milled and blended mix of clay and limestone which, after cooling, is blended with a few percent of calcium sulfate ($CaSO_4$, '$C\bar{S}$') to optimize the setting time and strength development of

the final cement [3, 1]. The chemical phenomena occurring during industrial production can be divided into three categories that take place in the following order:

(1) Reactions below 1300 °C (taking place in a preheater);

(2) Reactions at 1300–1450 °C (taking place in a rotary kiln);

(3) Reactions upon cooling (taking place in a cooler).

The material leaving the rotary kiln is referred to as the cement clinker. A photograph of cement clinker can be seen in Fig 1.

Figure 1. The product leaving the kiln is cement clinker granules of diverse sizes.

Traditionally, fossil fuels like oil, natural gas, pulverized coal, and lignite have been used for clinker production. For economic and environmental reasons these fuels are, however, often supplemented by waste materials such as industrial and municipal waste, as well as worn-out tyres. Some waste materials, i.a. blastfurnace slag, can also in fact be used in the raw feed, whereas flyash, for instance, can serve both as fuel and as a raw material.

Cement can be manufactured either in a wet or a dry process. For some raw materials the wet process is beneficial but, in most cases, the dry process is applied due to its higher thermal efficiency. In Europe, 90 % of the cement clinker comes from a dry kiln [20]. Therefore, the following description will be of the dry production process, illustrated in Fig 2. Here, it can be seen that the whole procedure takes between about two and nine weeks, and that the active processing of the material actually constitutes a very small part of the entire production.

Analyses of different kinds are continuously performed throughout the manufacturing process. Before going into the mixing bed, the bulk raw material can be analyzed by Prompt Gamma Neutron Activation Analysis (PGNAA), which is a non-destructive technique to define the elemental composition. In the raw mill, the PSD of the raw mix is measured and XRF measurements are often carried out. The clinker coming from the kiln

is usually analyzed with XRF and XRD, and the final cement is commonly evaluated by means of both XRF, XRD, and PSD. The physical lab provides possibilities for compressive strength measurements. For more details on the analytical methods, see the section *2.1.4 Tests and analyses*.

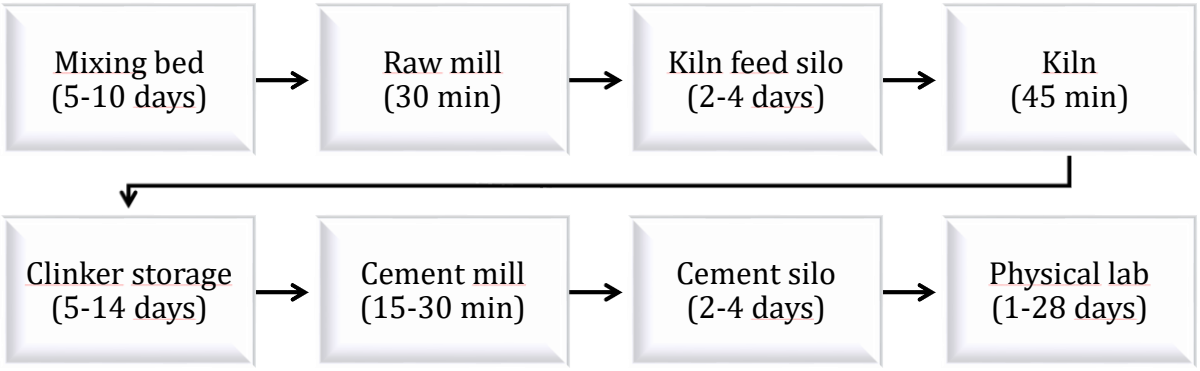

Figure 2. Flow chart of a classical Portland cement production with the residence time specified. It is worth noting that the actual processing of the material constitutes only a fraction of the entire production time; the materials spend most of the time in storages. The physical lab located at the end of the production is part of the product quality check.

2.2.1. Reactions below 1300 °C

Before entering the rotary kiln – the heart of the process – the raw meal goes through a preheater (mostly a co-current heat exchanger) where, within a minute, it reaches a temperature of about 800 °C. During this step about 40 % of the $C\bar{C}$ undergoes calcination to form C, while releasing $\bar{C}$:

$$CaCO_3(s) \rightarrow CaO(s) + CO_2(g) \qquad \Delta H = +2138 \frac{\text{kJ}}{\text{kg Portland cement clinker}}.$$

The large positive number of the reaction enthalpy, ΔH, indicates that this decarbonation is highly endothermic, i.e., very energy demanding.

Clay minerals are also decomposed, and calcite or lime reacts with clay mineral decomposition products and quartz (silica) to form C_2S, C_3A, and C_4AF, which, together with lime, are the predominant phases at the end of this process step.

Often, a precalciner is also used. The material then passes through a furnace chamber, in which a good 50 % of the fuel is burned. Up to 95 % of the calcite is decarbonated here and fuel ash is integrated into the material that exits the precalciner at a temperature of about 900 °C. The usage of a precalciner comes with many benefits; for instance, thanks to the efficient heat transfer in the precalciner, less heat is required in the kiln and the material can pass through the kiln at a significantly higher rate, thus lowering the capital cost. Due to the highly efficient heat transfer, the temperature within the particles is roughly the same as in the air, meaning that, in the precalciner, the chemical reactions are rate determining.

2.2.2. Reactions at 1300–1450 °C

From the precalciner the material is transferred into a rotary kiln, in which it is further heated to a final temperature of about 1450 °C – the clinkering temperature, T_{clink}. Here, in contrast to the precalciner, the heat transfer is slower and, hence, it is the rate determining factor. The aim in the kiln is to sinter the material, i.e., to partially melt it, to form clinker [4].

Most important is the formation of C_3S and there are two thermodynamic reasons behind the need for the high temperatures; firstly, C_3S, or leastways pure C_3S, is thermodynamically stable only above 1250 °C and, secondly, the endothermic nature of the reaction demands a temperature well above 1250 °C to achieve a driving force of Gibb's free energy (ΔG) large enough for the reaction to take place within a reasonable time frame in the kiln [15].

The rotary kiln itself is a slightly sloping tube (with a slope of 3–4 % from the horizontal) which rotates with 1–4 revolutions per minute and makes the material move from the inlet at the higher end towards the lower (front) end. At the front end, a flame is producing hot gases that flow in the opposite direction of the material feed which, in turn, is heated gradually until it reaches its maximal temperature close to the flame. In this region of the kiln, known as the burning, clinkering, or sintering zone, the material spends between 10 and 15 minutes. The flame must be adjusted so that the clinker is burned correctly. The aim is to minimize the amount of free lime to the lowest fuel consumption possible, while maximizing the C_3S concentration. If solid fuel is used, the ash from it has to be absorbed evenly by the clinker.

The main processes in the kiln are the following:

(1) C_3A and C_4AF (and some C_2S) melt;
(2) nodules are formed;
(3) free lime reacts with unreacted silica and C_2S to form C_3S:
$CaO(s) + SiO_2 + 2CaO \cdot SiO_2 \rightarrow 3CaO \cdot SiO_2$;
(4) C_2S undergoes a polymorphic change to its α-form;
(5) the C_3S and C_2S phases recrystallize and new crystals are formed;
(6) volatiles are evaporated.

At T_{clink}, 20–30% of the material mix is molten and the liquid consists mainly of C_3A and C_4AF. If SO_3 is in the raw material, at T_{clink} the majority of it constitutes an own liquid phase, immiscible with the clinker liquid. At equilibrium, the main phases present are C_2S, C_3S, and liquid. Magnesium oxide, MgO, can increase the reactivity and also enter the clinker liquid, together with the majority of alkalis (K_2O and Na_2O).

Nodulization occurs as a sufficient proportion of liquid is present and it denotes solid particles getting stuck together by liquid. This process is favored by small solid particles and a low-viscous liquid with a high surface tension. It is also linked to the chemical reactions and evaporation of volatiles (like alkali sulfates, halides, and hydroxides, SO_2 and O_2) taking place. The material undergoes compaction and is transformed from a state of large local compositional variations to constituting a more continuous matter, all while C_3S is being formed.

The optimal size of an C_3S crystal, from a 28-day strength point-of-view, is ~15 µm as this provides the right number of defects and, hence, reactivity (larger crystals hold less defects and are therefore less reactive). The crystal size is affected by the heating rate up to T_{clink}, as well as the time and temperature in the burning zone. In practice, however, not many clinkers have an average C_3S crystal size of 15 µm.

It is usually stated that the conditions should also be oxidizing, so that the majority of the iron in the cooled clinker will be in the form of Fe^{3+}. In reality, however, the majority of iron is present as Fe^{2+} in the kiln and converted to Fe^{3+} only during cooling. Reducing conditions can appear locally within the material in the burning zone of the kiln due to lack of oxygen in the kiln gas, reducing material present in the raw meal, or trapped solid fuel particles. The effect of reduction can be tangible as C_3S is easier decomposed and less C_4AF is formed in favor of C_3A. If other reactions occur parallel to the reduction, this generally has a negative impact on properties like strength development and setting time of the final cement.

Burnability, previously discussed in the section *2.1.3 Quality assurance and parameters* is used to describe the ease with which the amount of free lime within the raw mix can be reduced to a desired level in the kiln. However, as the reaction rate of the free lime is not solely determined by the mix properties, but also on the treatment and conditions before and in the burning zone itself, burnability can only be defined for a given kiln with a particular set of operating settings. Generally, though, a higher LSF or SR gives a lower burnability, as this implies more CaO in need to react, and less liquid available at a given temperature, respectively. The particle size plays a role – especially coarse particles in the raw material affect the time to burn the clinker – just as factors like microstructure, containment of minor components, and how intimately the raw materials have been mixed.

2.2.3. Reactions upon cooling

Clinker nodules, with a typical diameter of 3–20 mm, are formed in the burning zone while in a semi-solid state. The subsequent cooling, beginning already in a cooling zone within the kiln, makes the nodules solidify entirely. When leaving the rotary kiln, the inner temperature of the nodules is around 1350 °C but the surface is considerably cooler. Rapid cooling (air-quenching) right after the burning zone is important for high-quality clinker and when entering the grinding mill, the temperature should be below 1100 °C.

There are different systems for clinker cooling with grate coolers representing the latest technology that has proven to offer the most efficient heat recovery compared to other cooling techniques [21]. As the hot clinker holds a significant amount of heat, an effective cooling system is an important key in lowering the production costs [21].

As already mentioned, the large share of iron prevailing in the form of Fe^{2+} after leaving the burning zone, is oxidized to Fe^{3+} during cooling. In fact, it is this oxidation of C_4AF that determines the color of the final Portland cement clinker, which is typically almost black – the more oxidation, the darker the clinker.

The reactions taking place during cooling are affected both by the composition (above all, the AR is important) and the cooling rate. The clinker liquid can crystallize either in a continuous equilibrium with a material transfer with the solid C_3S and C_2S phases present, or independently with no liquid-solid exchange of material. There can also be a combination of the two crystallization types – it all depends on the kinetics defined by the applied cooling rate and current temperature. Glass formation requires such rapid cooling that, in practice, it does not occur in ordinary clinker production.

The structure and the composition of the C_3A and C_4AF phases, also, both depend on the cooling rate. For example, slow cooling yields larger crystals and vice versa, and the degree of crystallinity varies with the rate of cooling. Furthermore, the allocation of the atoms into tetrahedral and octahedral C_4AF sites is predicted by the prevailing temperature at the time of internal equilibration within the crystal. These are some things that may influence how the interstitial material behaves later on hydration.

Polymorphic transitions of the C_3S and C_2S phases occur during cooling. Also here, the cooling rate plays a role, both on the C_2S transitions, and on the C_3S crystal size; faster cooling gives smaller crystals which makes the clinker easier to grind. According to studies made, faster quenching of C_3S, likely also leads to more crystal defects, resulting in shorter induction periods [22]. A too low cooling rate at temperatures between 1250 °C and 1100 °C cannot just negatively impact the crystal size, but actually cause the C_3S to decompose. The presence of Fe^{3+}, sulfate melts and water vapor further accelerate this process, while Mg^{2+} significantly retards it.

In the kiln, alkali cations are distributed between the clinker and sulfate liquid and the C_3S and C_2S phases. When the temperature then sinks below 900 °C, the sulfate liquid starts to solidify forming mainly K_2SO_4 and $K_{4-x}N_x\bar{S}_4$, with x between 1 and 3. As the solid sulfates arise quite late, their crystals usually end up between the silicate phases. If, however, the clinker mixture is rich in SO_3, the sulfates may partly emerge as inclusions within the silicates.

Impurities in C_3S, mainly Al and Mg, further stimulate grain growth throughout cooling.

In a summary, it is desirable to keep a high cooling rate; finer C_3A grains closely mixed with C_4AF react slower with water, enabling a better control of the setting rate, the C_3S content is better maintained, the clinker is easier ground, and also, a larger content of MgO can be tolerated.

2.2.4. Grinding and calcium sulfate addition

Grinding takes place on two occasions during cement production – firstly, when mixing the raw materials and, secondly, when milling cool cement clinker. Together these two processes consume about 65 % of the entire electrical energy used in a cement factory and the clinker grinding alone accounts for approximately 40 % of the total electrical energy used [23].

Grinding aids – diverse kinds of surfactants – can be added to reduce the energy demand by mainly counteracting agglomeration. The surfactants are absorbed by the anhydrous

phases. Modern grinding aids are formulated to also affect properties like setting time and early strength development.

Calcium sulfate ($CaSO_4$) is always added in the clinker grinding step – either as gypsum ($CaSO_4 \cdot 2H_2O$ or $C\bar{S}H_2$), anhydrite ($CaSO_4$ or $C\bar{S}$) or as a combination of the two [17]. It is at this stage that the clinker actually turns into cement. Sulfate (SO_3 or $\bar{S}$) is a set-controlling agent which acts by balancing the C_3A phase upon hydration and with that, it also impacts the strength development. As described previously in the section *2.1.2 International standards*, the SO_3 content should be neither too low nor too high to avoid flash and false setting respectively. Sulfate optimization is therefore also an essential part of the grinding process. This is most easily accomplished through a gradual SO_3 supply combined with regular sampling and measurements of the SO_3 content and corresponding parameters like setting time and strength [17]. The SO_3 optimum is seldomly the same for the various parameters and so, SO_3 optimization is typically done in regard to the most important parameter for the purpose [17].

The clinker milling process has two parts – 1) crushing of larger grains into a powder and 2) grinding of the powder to the particle size desired. Here, the clinker goes from millimeter size to being measured in micrometers [17]. There is a wide variety of different mills, both when it comes to size and function. There are, for example, roller presses, ball mills and spindle mills, of both open and closed-circuit type. In open circuit mills the clinker is ground in batches, until the specified average surface area is reached [17]. This has the effect that softer cement components will be ground to a remarkably fine powder while waiting for the harder parts to get sufficiently small. One way around this, is to use a closed-circuit mill, in which the finer powders are separated, while coarser materials are brought back for a new round of grinding. This procedure increases efficiency and generates a product with a narrower PSD [17]. A drawback of the latter is, however, a decrease in workability, as the increase in void space between the particles enhances the need of water to fill the voids. From this perspective, the presence of finer ground material is advantageous, and limestone is often added to fill the empty spaces.

In summary, the grinding process is highly important for the final cement quality. The procedure cannot be adjusted to compensate for poor clinker quality but, if conducted in an improper manner, also good clinker can be turned into a low-quality product [17].

2.3. Cement hydration

The term *cement hydration* embraces the entirety of transitions that take place when an anhydrous cement – or any of its individual phases – is blended with water. It is a complex process, which not only includes the conversion of anhydrous substances into their analogous hydrates but holds many different reactions, which take place simultaneously, in series or in a complex combination. These reactions can be categorized as either dissolution, diffusion, growth (attachment and incorporation), nucleation, complexation (ion reaction), or adsorption processes [22]. Together they generate three main products: calcium silicate hydrate (C–S–H), calcium hydroxide (CH), AFt and AFm (aluminate ferrite, tri- and monosubstituted respectively).

The complexity of the material makes it difficult to isolate and study individual chemical reactions within the progress of hydration. For kinetic studies it is therefore common to examine the net rate of hydration, which covers the totality of the progress without taking individual processes into account [22]. There are several techniques suitable for this, for example isothermal calorimetry, nuclear magnetic resonance spectroscopy (NMR), in situ quantitative XRD, and small angle neutron scattering (SANS). None of these techniques can be used to find details regarding specific mechanisms, but they are useful for comparisons of the hydration of different cement types and to study the impact of parameters such as cement composition, presence and content of admixtures, and particle size [22]. It has also proved useful to run parallel experiments with different techniques (for example SANS and calorimetry) and then compare and correlate these. In the case of a combined SANS-calorimetry measurement, as an example, it can then be seen, how the surface area behaves in relation to the measured heat development.

When cement and water are mixed in the right proportions, a cement paste is formed, which can undergo subsequent setting and hardening. It is worth noting that the hardening process of the cement is not a consequence of the material drying, but a chemical reaction in which the water takes part in forming bonds [1]. As the material *sets,* it stiffens without developing any significant compressive strength. Instead, the compressive strength grows as the material *hardens*. Initially, the water-cement reaction only takes place on the surface of the grains and, hence, this is where the strength-providing hydration products form [17]. Consequently, at an early age, the larger the surface area, the stronger will the cement be.

Typically, the so-called water/cement or water/solid ratio, abbreviated w/c, and w/s ratio respectively, should be somewhere between 0.3 and 0.6 in respect to the mass.

Three main stages of reaction can be defined for the hydration process: 1) *the initial reactions,* 2) *the induction period*, and 3) *the main reactions*, which include both an acceleration and a deceleration period. The heat development varies considerably between the different phases of the process, which is why isothermal calorimetry is so useful in following the progress of hydration (the technique is described in more detail in the section *3. Isothermal calorimetry*).

In the calorimetric curves in Fig 3, the three stages of hydration are displayed with approximate time indications. This particular measurement was conducted for only 18 but the main reaction continues for much longer than that. The thermal power will continue to gradually decrease as the system moves into a phase of a slow long-term reaction, which can proceed up to several years, depending on the particle size and the availability of water.

As briefly mentioned in the section *2.2.4 Grinding and calcium sulfate addition*, sulfate is important for balancing the C_3A reactions on hydration. If sulfate remains unreacted in the hydrated paste, this can lead to later formation of ettringite (further depicted below), which is associated with an expansion of the material. Therefore, the sulfate levels should ideally be such, that they deplete not too long after the main reaction peak. If sulfate is depleted before the hydration process has reached its maximal rate, this can lead to aluminum poisoning, where free Al^{3+} ions in solution can hamper the C_3S reaction. The

curve in Fig 3 has a shoulder on the right side of the main peak indicating a beginning of sulfate depletion. Such shoulders can, however, emerge without being connected to the sulfate levels in the sample.

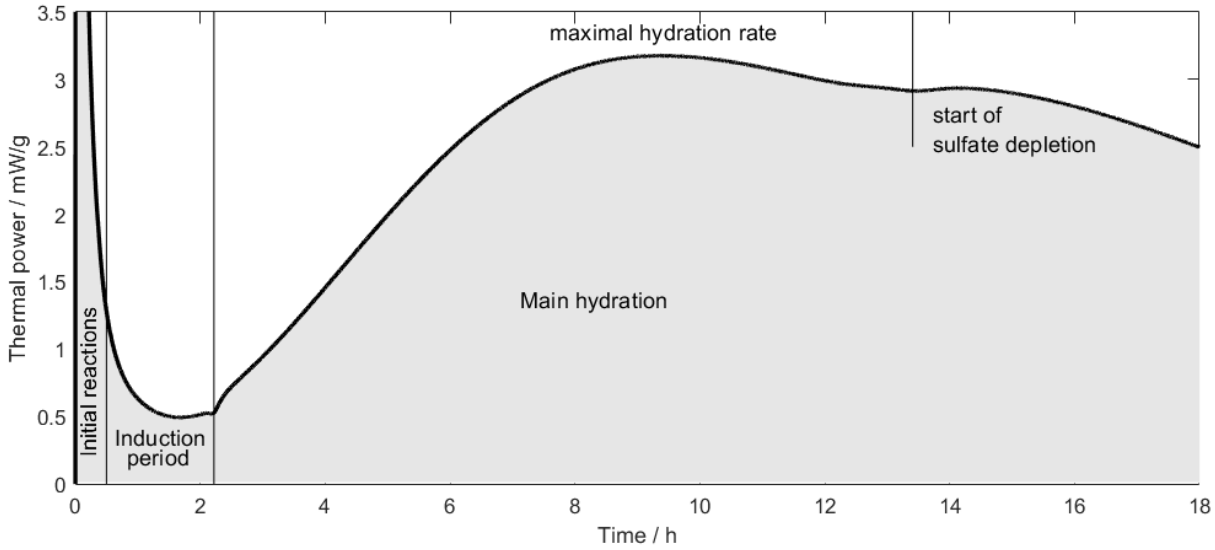

Figure 3. A calorimetric power-time curve showing the development of thermal power resulting from cement hydration.

The main reaction mechanism of cement hydration is a combination of dissolution and precipitation; the anhydrous minerals dissolve into ions and then form new (hydrated) compounds while precipitating. The dissolution process can be congruent or incongruent. Congruent dissolution refers to the mineral dissolving completely into its constituent ions, whereas an incongruently dissolving mineral dissolves only partially while a solid weathering product is left behind [24].

2.3.1. Hydration products

For the part on hydration products, the book section *4 - Constitution and Specification of Portland Cement* written by A. M. Harrisson in *Lea's Chemistry of Cement and Concrete (Fifth Edition)* [17] has been used as reference, with a few exceptions that are separately indicated.

As already mentioned above, the main products of cement hydration are C–S–H, CH, AFt and AFm. Calcium silicate hydrate, $CaO - SiO_2 - H_2O$ or C–S–H, is a major product formed when C_3S and C_2S react with water. It is often referred to as a gel instead of a crystal since no apparent regular structure has been found in XRD analyses. As the denotation indicates, the C–S–H gel has no consistent stoichiometry but, the amount of CaO is typically about twice the SiO_2 content. In fact, the CaO/SiO_2 ratio of C–S–H is near the one in C_2S and, consequently, hydration of C_2S mostly leads to C–S–H formation:

$$Ca_2SiO_4 + H_2O \rightarrow CaO - SiO_2 - H_2O$$
$$(C_2S + H \rightarrow C - S - H).$$

In case of C_3S though, there is more CaO present, which makes it more reactive than C_2S and causes C_3S hydration to, in addition to C–S–H, also produce calcium hydroxide:

$$Ca_3SiO_5 + H_2O \rightarrow CaO - SiO_2 - H_2O + Ca(OH)_2$$
$$(C_3S + H \rightarrow C - S - H + CH).$$

As discussed in earlier sections, cement clinker always contains some free lime, and this also forms CH when reacting with water:

$$CaO + H_2O \rightarrow Ca(OH)_2$$
$$(C + H \rightarrow CH).$$

If no sulfate is present, C_3A, reacts with water in the following way:

$$2C_3A + 21H \rightarrow C_4AH_{19} + C_2AH_8.$$

This is the reaction of flash set, which denotes the fast hardening of the paste occurring due to the irreversible formation of calcium aluminate hydrates shown above.

Addition of sulfate to the system changes the initial reaction towards the production of a calcium sulfoaluminate hydrate called ettringite. If SO_3 comes in the form of gypsum, the modified reaction is:

$$C_3A + 3C\bar{S} + H_2 + 26H \rightarrow C_6A\bar{S}_3H_{32}.$$
$$(\bar{S} = SO_3, H = H_2O).$$

Ettringite is also denoted AFt or tri-sulfate, where A and F stand for Al_2O_3 and Fe_2O_3 respectively, while the t represents three moles of calcium sulfate. As long as all the reactants are accessible, ettringite will keep forming but, if the system runs out of sulfate, AFt can give off two moles of calcium sulfate and undergo a transition to AFm – mono sulfo-aluminate hydrate.

As the hydration of the C_4AF phase is barely mentioned in the literature found, it has been deliberately omitted from this report.

The hydration enthalpies for the four major cement phases are summarized in Table 2. The values presented, clearly show that the reaction of C_3A is the one mostly contributing to the heat output, calculated per mass. These numbers certainly say nothing about when in the process this heat is developed, but generally one can see that a higher C_3A content causes an overall increase in heat of reaction.

Table 2. Enthalpies of the complete hydration of the four main phases of cement. The values have been retrieved from P. D. Bentz [25].

Phase	C_3S	C_2S	C_3A	C_4AF
Enthalpy (kJ/kg phase)	517	262	1144	725

2.3.2. Initial reactions

For the following part on initial reactions, the induction period and the main reactions, the article *Mechanisms of cement hydration* by Bullard, Jeffrey W., et al. [22] has been used as reference, with a few exceptions that are separately indicated.

The initial reactions begin as soon as the cement is exposed to water. This stage is mainly defined by C_3S and C_3A reacting rapidly with water, which can be linked to a dramatic increase in the calorimetric power-time curve. The major hydration product being formed during the initial reactions is ettringite ($C_3A \cdot 3CaSO_4 \cdot 32H_2O$). Within just a few minutes, the C_3A reaction rate falls again to enter a period of lower heat production.

The C_3S dissolution occurs congruently and in just a few seconds after wetting, according to:

$$C_3S + 3H_2O \rightarrow 3Ca^{2+} + H_2SiO_4^{2-} + 4OH^- \qquad \Delta H = -138 \text{ kJ mol}^{-1}.$$

The solutes then start precipitating as a C–S–H [26].

2.3.3. Induction period

C_3S

The rate of C_3S dissolution decelerates quickly before the solution gets saturated, for reasons that are not completely understood. There are several probable explanations for this. One of these is the *metastable barrier hypothesis*, according to which a metastable calcium silicate hydrate layer, (C–S–H (m)) could be limiting the water access of the cement particles or preventing the dissolving ions from diffusing away from their surface. The hypothesis indicates that the underlying isolated C_3S and the hydrate come into a state of equilibrium. The theory does not provide any clear explanation on what actually would cause this delay period to end, but the highly repeatable time value could imply some type of chemical reaction finally degrading the metastable layer. This is also consistent with calorimetric measurements exhibiting a low but non-zero heat flow during this somewhat retarded period.

Even though the metastable barrier hypothesis is frequently recurring in literature, its validity has been a subject of debate. According to Scrivener and Nonat [26] it has, in fact, not been possible to demonstrate the existence of such a layer. They also state that the profound difference in atomic structure between C_3S and C–S–H makes it rather unlikely that the latter would surround the former with a nearly impermeable layer. Instead, they argue that the induction period is linked to the C_3S dissolution rate. This *slow dissolution step hypothesis* implies that the initial driving force for the dissolution is high due to undersaturation of the water but that this decreases gradually as the water gets more and more saturated by dissolution products, causing the reaction to slow down [26]. Just as for many other natural low-solubility minerals, C_3S has different dissolution mechanisms, and it is the saturation of the aqueous solution that determines, which of these mechanisms that is rate controlling at a given point; when the system is far from equilibrium dissolution occurs at a higher rate due to a stronger thermodynamic driving force enabling opening of etch pits at surface defects. When approaching equilibrium, but still in a clearly undersaturated state, the driving force declines, and dissolution is

governed by a significantly slower retreating step mechanism. It can also be mentioned that the rate of the clinker cooling plays a role here, as faster quenching induces more crystal defects, whose presence has been shown to shorten the induction period.

It is not completely clear when the formation of stable C–S–H gel actually occurs and if it is necessarily preceded by a metastable C–S–H layer as described in the metastable barrier hypothesis. Per definition, an induction period denotes the time before the first nucleation, but if C–S–H is actually already growing slowly at this point, Bullard et al. state that it might be better to talk about this as a delay rather than an induction period. ^{29}Si NMR studies suggest that silicate starts to polymerize at the end of this period of slow reaction, which may indicate that silicate polymerization is important in the shift to the kinetics of nucleation and growth.

C_3A

As mentioned above, the C_3A reaction rate falls within a couple of minutes after wetting. The available amount of calcium sulfate defines the length of the subsequent low-heat period and as soon as the calcium sulfate is all consumed, the reaction picks up speed again and starts to mainly generate calcium monosulfoaluminate. Ideally this slow-reaction period of C_3A should extend well past the main hydration peak to secure a proper setting and hardening.

The exact mechanism behind the retardation of the reaction is not clear, but there are several possible explanations, including a hypothesis of an ettringite diffusion barrier being formed at the surface of C_3A. Another suggestion is that sulfate ions might adsorb to C_3A surfaces, and to sites of crystal defects in particular, thereby preventing etch pit formation and retarding the dissolution process. If this latest approach is correct, this could explain why the reaction rate falls more rapidly in the presence of the more readily soluble hemihydrate, than when the more insoluble $C\bar{S}_2$ is used as sulfate carrier.

2.3.4. The main reactions

In literature, many different possible mechanisms can be found that could explain the transition from the low-reactive induction period to an acceleration of the hydration rate. It is however clear that the increased reaction rate is associated with a simultaneous formation of C–S–H and CH, and that the main hydration peak predominantly is a result of C_3S and C_3A reactions [27].

One possible mechanism is a rupture of the metastable C–S–H barrier described in the *metastable barrier hypothesis*. If Ca^{2+} and water can pass through this barrier, while silicate ions are held back, this would cause silicate to accumulate and form a swelling gel, that would exert a pressure on the barrier and finally lead to a rupture of this. As the silicate ions are set free and face the Ca^{2+}-rich solution, this would then enable fast C–S–H formation.

In later research papers this hypothesis is, however, often rejected. Other, frequently recurring theories are instead focusing on dissolution and 'nucleation and growth' (N+G), for which

so-called 'N+G models' are used – models that fit closely with the data relating to the main reaction peak [28]. Assumptions made, are based on a relatively constant driving force for the nucleation and growth processes around the main peak [28]. During the acceleration of the main reactions, CH, and C–S–H grow with an increasing rate, and this also controls the rate of C_3S dissolution [28].

As described by Scrivener and Nonat [26], the hydration process is heterogeneous as it includes one liquid phase and at least two solid ones – minimum one unreacted anhydrous phase and hydrated phase. Therefore, the balance between the dissolution and precipitation rates of the different minerals plays a crucial role in determining the phases being formed, and this type of reactions is thus dependent on the area of the solid-solution interface. At the beginning the area of the growing phase is zero and, by the end of hydration, the area of precipitating phases is zero. Since the precipitation of hydrated phases relies on dissolution products from the unreacted phases, most of the time, the overall rates of the respective processes are approximately the same but the interfacial rates of dissolution and precipitation (given in mol m^{-2} s^{-1}) are constantly changing [26]. On a macroscopic level, the maximal hydration rate is reached when the surfaces of the dissolving and precipitating phases are identical [26].

All this is also linked to the Gibbs free energy of reaction, ΔG, denoting the thermodynamic driving force for these reactions to occur. It is good to keep in mind that the solubility varies among the different phases, which means that the ion concentration affects the reactions to different extents.

After the main peak, the rate of hydration continues to decrease but the reaction goes on, and within 28 days, 70 % of the C_3S has reacted.

Thermochemistry, thermodynamics, kinetics, and mechanisms

The interdependence of the microstructural and chemical phenomena makes it hard to grasp the reaction mechanisms on an individual basis and thus, to resolve the kinetics-determining factors of these [22]. The development of appropriate techniques and methods for experiments and modeling is a challenge. At the same time, the work towards more sustainable cements stimulates the creation of more complex mixtures with industrial by-products and, in order to better understand the consequences of different mixture proportions, it is crucial to know the basic mechanisms of hydration and their kinetics.

In serial reactions, one reaction uses the product of the previous reaction as a reactant. According to Bullard et al. [22], it is common for one reaction step to be slower than the others and thereby control the rate. This step is then determining both the kinetic rate equation observed, as well as the rate constant and the impact of temperature. When, on the other hand, no single reaction step can be outlined as rate-controlling and there, instead, are two or more reaction steps with similar rates prevailing, then both the rate equations and the influence of system parameters easily become more convoluted and harder to deduce from experiments.

Furthermore, it is difficult to adequately define the surface at which certain reactions take place, and to know the particle size distribution and the absolute area of the surface, which is a prerequisite to generate appropriate rate data [22]. Resultantly, the net effects of the hydration kinetics of Portland cement are only partly known. A solution to this would be to study the rates of the main individual processes separately.

The majority of studies of the kinetics of Portland cement hydration, mainly focuses on the hydration of C_3S [22]. As this phase constitutes 50–70 mass-% of the cement, it is an uncomplicated way to get a basic understanding of the process; the complexity of the analysis increases rapidly with more components and phases involved. Also, the early period of hydration – which includes both setting and the early development of compressive strength – is predominantly ruled by C_3S hydration. Another option is to use pure C_3S for the kinetic analysis. It is, however, important to be aware of the differences between the two materials and, hence, the possibly different results generated from their respective hydrations. There are speculations that the differing crystal structures of the materials and the prevalence of impurities, in fact, can have an effect on the number of reactive sites, such as stacking faults and screw dislocations, at the grain surface, which in turn would alter dissolution [22]. Even the hydration products seem to differ; the C–S–H in the pure C_3S paste has been proved to be denser and, thereby, to a larger extent counteract mass transport.

3. Isothermal calorimetry

Chemical reactions, of all kinds, are closely connected to the concept of energy in general and heat in particular. Instruments for heat measurements have, therefore, long been of large interest. One of the earliest devices for this purpose was constructed in 1780 by Lavoisier and Laplace [29]. It was an ice calorimeter, which used melting ice to quantify the heat released from different objects and processes. Ever since, several types of calorimeters have been developed for various purposes. The focus here will be on isothermal calorimetry – a technique that is very well suited for measurements on cement samples [30].

Heat, just as other forms of energy, is measured in Joule (J) and studying the heat development over time is a way to gain understanding of reaction kinetics and essentially the reaction rate.

An isothermal calorimeter is a device enabling measurements of the heat production rate of a process. This heat rate is also named *thermal power*, denoted *P,* and, since it is a measure of an energy flow, it is given in J/s=W. For practical reasons, however, it is often more convenient to present it in units of mW or μW.

The output generated from these measurements is the specific thermal power (P/m) in units of W/g_{sample} versus the time, t. Scaling the results with the sample mass allows the comparison of different samples and integration of the thermal power gives the total heat of reaction, Q, in J/g_{sample}. The amount of heat produced is proportional to the extent of reaction or, in case of cement hydration, the degree of hydration, α. For cement the produced heat can be up to 450 J/g.

3.1. The isothermal heat conduction calorimeter

The significant feature of an isothermal calorimeter is its ability to work at a constant, preset temperature. The instrument has the following six main compartments:

(1) *Insulation* and a *thermostat* to ensure a thermostated environment;

(2) A thermostated *heat sink* (metal block) used to keep the temperature stable;

(3) A *sample heat flow sensor* recording produced heat that flows through it;

(4) A s*ample ampoule holder*;

(5) A *reference heat flow sensor*;

(6) A *reference* – an inert material similar to the sample with the same heat capacity.

The sample to be studied is loaded in an ampoule, which for cement and mortar samples can be made of either glass or high-density polyethylene [31]. When exothermal or endothermal heat is produced in the system, the temperature change will cause heat to flow [30]. This gives rise to a temperature difference, which is then registered as a voltage by the heat flow sensor.

3.1.1. The reference

No matter the quality of the thermostat and the insulation, there will still always be disturbances coming into the thermostated environment and, for this reason, a heat conduction calorimeter always has a reference system with an inert sample [30]. It provides noise reduction and an improved kinetic response. Due to this, it is crucial for the measurements and the absence of a reference can, in fact, make it impossible to interpret the measured results.

As mentioned above, the refence is chosen to match the thermal properties, including the heat capacity, of the sample. Usually, simple materials like water, quartz, or stainless steel are used. When disturbances occur, these will influence the sample and the reference simultaneously and to the same extent. The reference signal, U_{ref}, is detected and then subtracted from the sample signal, U_{sam}. Accordingly, the output signal, $U = U_{sam} - U_{ref}$.

3.1.2. The baseline

Ideally, the absence of heat flow from the sample should result in a zero signal. However, by cause of small amounts of heat produced by, for example, electronics within the instrument, the signal at zero thermal power will always be unequal to zero. This offset from the zero line is known as the baseline U_0 (V). It is necessary to subtract the baseline, especially before integration of the thermal power when calculating the heat.

Baselines are determined by conducting an at least 24-hour measurement with equal heat capacity in the sample and reference positions.

3.1.3. Calibration and calculations

The primary output from a heat conduction calorimeter is an electrical voltage, *U,* in units of V. In order to convert this to thermal power, the voltage is multiplied by the calibration coefficient, ε, which has the unit W/V, according to:

$$P = \varepsilon * U \tag{1}$$

Ideally, calibration coefficients should be measured before and after measurements, and maybe in between, as they are essential for the data analysis. Generally, ε is stable but in rare cases there can be some cracks in the heat flow sensors or other problems in the instrument causing gradual change in how the instrument reacts to thermal power, which will not be noted without calibration.

The most common calibration method is electrical calibration [30], in which the response of an electrical current, I (A) conducted through a heater (resistor) with resistance R (Ω) is assessed. The thermal power generated by the calibration heater can be calculated by:

$$P = I^2 R \tag{2}$$

The current can either be applied until a steady state is reached or it can be turned on and off as pulses of, for instance, 10 min. If pulses are used, the input is the electrical thermal power, P, with a curve in shape of a rectangle. The curve of the output voltage, U, however, normally exhibits a rising and falling exponential behavior due to the thermal inertia of the system. A pulse calibration with a pulse duration of Δt (s) the following equation is used to determine ε:

$$\varepsilon = \frac{P \cdot \Delta t}{\int U \, dt} \tag{3}$$

A steady-state calibration, on the other hand, does not require an integration. Instead, for this case, ε can be calculated by simply rearranging equation (1), which means that:

$$\varepsilon = \frac{P}{U} \tag{4}$$

Both calibrations are pictured in Fig 4.

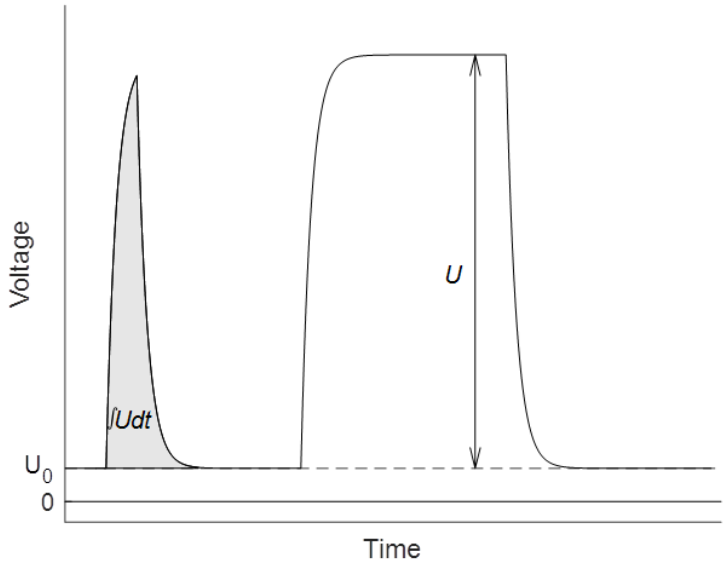

Figure 4. The output voltage generated from an electrical calibration plotted against time. To the left a pulse is applied, requiring an integration of the voltage curve. To the right a steady state is reached before the value of the voltage can be used for calculating the calibration coefficient ε.

Optimally, electrical calibration should also be combined with chemical calibration made in a way similar to the measurements being conducted [32]. For this a well-known chemical reaction is needed with a known amount of heat being produced. The value of ε generated in the electrical calibration is then validated chemically; if the right heat of reaction is received, this confirms that ε is correct and that the measurements have been performed in a proper way. For cement hydration, there are two commercial calibration cements that can be used for chemical calibration.

The specific thermal power P_0 of a sample with the mass m can then be calculated from the voltage according to:

$$P_0 = \varepsilon \frac{(U - U_0)}{m} \tag{5}$$

However, heat transfer limitations within the sample and the instrument shows up an inherent thermal inertia. This means, that the generated raw data contains only the recordings of the sample heat flow sensor. To obtain a fair picture of the true heat development in the sample in studies of rapid reactions, the raw data, consequently, needs to be corrected for this time lag [30]. The Tian equation is a model using one time constant τ (s) to do exactly this:

$$P = P_0 + \tau \frac{dP_0}{dt} \tag{6}$$

The time constant τ can, for example, be calculated from the exponentially decreasing output signal coming from turning on the calibration heater during a brief period of time [30]. Note that the time constant is a function of the thermal properties of both the sample and the instrument, so a proper time constant can only be measured with a sample (or with a reference material with similar heat capacity) in the sample ampoule.

Finally, the thermal power, P, can be integrated between two points in time, $t_1$and t_2, to determine the overall heat Q:

$$Q = \int_{t=t1}^{t2} P\, dt \tag{7}$$

The manual calorimeter used in this project, was an I-Cal Ultra from Calmetrix (Fig 5). It is an eight-channel isothermal calorimeter enabling measurements of samples with volumes of up to 20 mL. The cells are thermostated and well isolated thanks to an air gap, which cancels the risk of the individual samples disturbing one-another (so-called cross talk). The thermostat works within the range of 3–90 °C and a stability of +/- 0.01 °C (31). A schematic illustration is shown in Fig 6.

The I-Cal Ultra is mainly used within the field of binders and complies with both the European and North American standards for testing on cement and other hydraulic materials.

Figure 5. The Calmetrix I-Cal Ultra isothermal calorimeter provides eight channels for individual measurements [33].

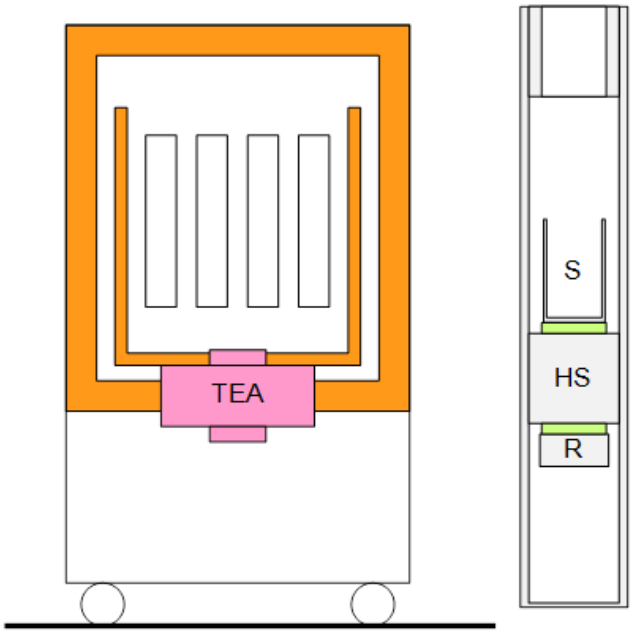

Figure 6. A schematic drawing of the I-Cal Ultra isothermal calorimeter. To the left is a cross section of whole instrument and to the right is one calorimeter. Orange colored parts are insulation, and the green devices are the heat flow sensors. TEA (thermoelectric assembly) is the thermostating device, HS is the heat sink, S is the sample vial holder, and R is the reference.

3.2. Calorimetric measurements of cement hydration

With isothermal calorimetry gaps between reactivity, compressive strength, and thermal power can be bridged; shifts in the calorimetric power-time curve correspond to changes in reactivity and can therefore complement both compressive strength measurements and quantitative XRD [10]. The latter provides only mineralogical data, which requires experience for anticipating the actual reactivity [10].

When studying cement hydration, it is most common to first prepare the sample, i.e., mix dry cement powder with water ex-situ, and then charge it in the calorimeter [31]. As the sample often is at a different temperature than the calorimeter, this will always give an initial thermal disturbance in the measurement. One way to avoid this effect is to use in-situ mixing, where the water is injected internally in the calorimeter. By doing it this way, both the sample and the water have had time to be thermostated and the heat development can be detected directly from the time of injection, thus enabling the examination of the early hydration reactions appearing in the initial peak.

A mixing vessel associated with the I-Cal Ultra is shown in Fig 7. It allows in-situ mixing of the samples. When preparing a measurement, the dry cement (clinker) is weighed into the 20 mL vial; the injection water and any additives are loaded into the syringes. The vial and the syringes are then lowered into the instrument, while the upper part of the mixing vessel is still sticking out of the calorimeter. Thus, the sample and the injection liquid can be thermostated before they are mixed. The externally operated electrical motor drives an L-shaped mixer, which facilitates the formation of a homogeneous cement paste.

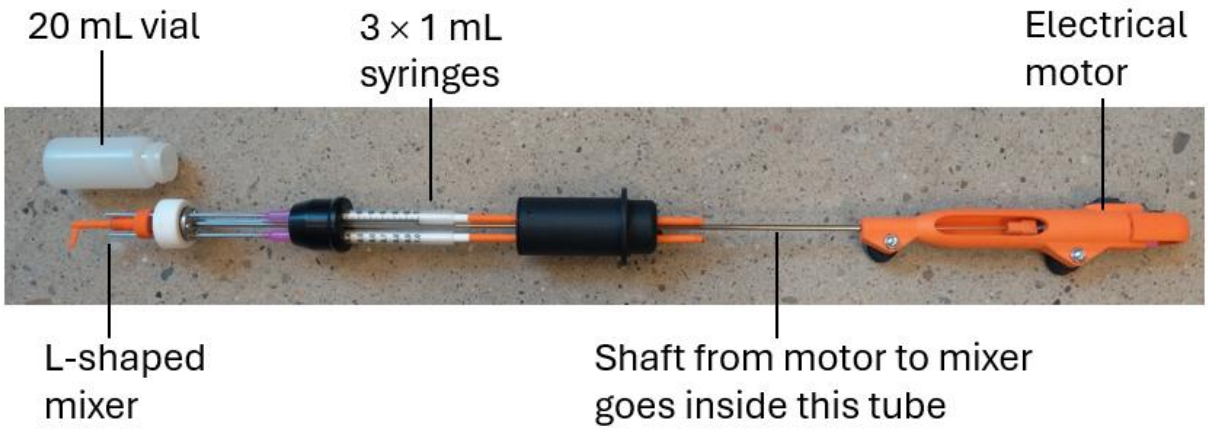

Figure 7. The mixing vessel has an L-shaped mixer powered by an electrical motor. During measurements, the vial and the syringes are hidden in the calorimeter, which allows for both the sample and the injection liquid to become thermostated before the injection is carried through under in-situ mixing.

However, there are two disadvantages of in-situ mixing vessels – firstly, the mixing is quite weak and, secondly, one can only assess the mixing quality after the measurement is finished.

3.3. Automated calorimetry – the polabCal

The polabCal is an automated calorimeter developed in cooperation between thyssenkrupp Industrial Solutions and Calmetrix. It is probably the first commercial fully automated isothermal calorimeter and was designed to enable and facilitate continuous automated quality controls within, among others, the cement industry. The purpose of the equipment is to, quickly and smoothly, provide relevant and accurate information on the reactivity of cement clinker and cement. By feeding this data back to the production, a more consistent product quality can be achieved – something that is highly desirable. By automating the laboratory work, the polabCal is meant to make important data more easily accessible and facilitate process-related decision-making.

If incorporated in a lab automation system, the polabCal can automatically receive samples from this directly. It is also possible to load the samples manually in a turntable magazine (Fig 8). The rest of the sample preparation is, however, completely automated – everything from sample weighing (Fig 9) and water addition (Fig 10), to mixing and insertion into the calorimeter. The mixing is conducted ex-situ in a high-shear vibrating mixer before the ampoule is placed in the calorimeter – an I-Cal Ultra, which is the same type of instrument that was used for the manual mixing vessel measurements. It takes about 75 s from the point of water addition to the point, at which the sample is in the calorimeter and the calorimeter starts recording the heat flow signal.

Figure 8. In the turntable magazine, samples can be loaded manually.

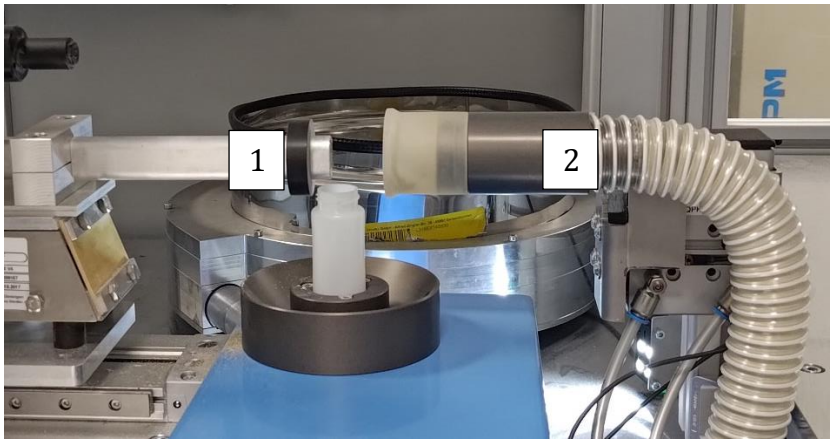

Figure 9. The samples are weighed automatically on a scale and the weight is recorded. The ground cement (clinker) is poured from the pipe to the left in the picture (1) and excess dust is removed by vacuum through the hose to the right (2).

A consequence of the ex-situ mixing is the loss of the early hydration kinetics, but as the delay is constantly reproduced, the initial peak recording can still be considered dependable. The heat produced in the sample before it is placed in the calorimeter is mainly retained in the vial as an elevated temperature and so, it is only the kinetics of the first 75 s that is lost.

A unique aspect of polabCal is that the enclosure that houses the robot and all the equipment needed to prepare the samples, has the same temperature as the calorimeter to within a few 0.01 K. Because of this, there will be no initial disturbance from the temperature difference between sample and calorimeter, as there is in normal ex-situ measurements.

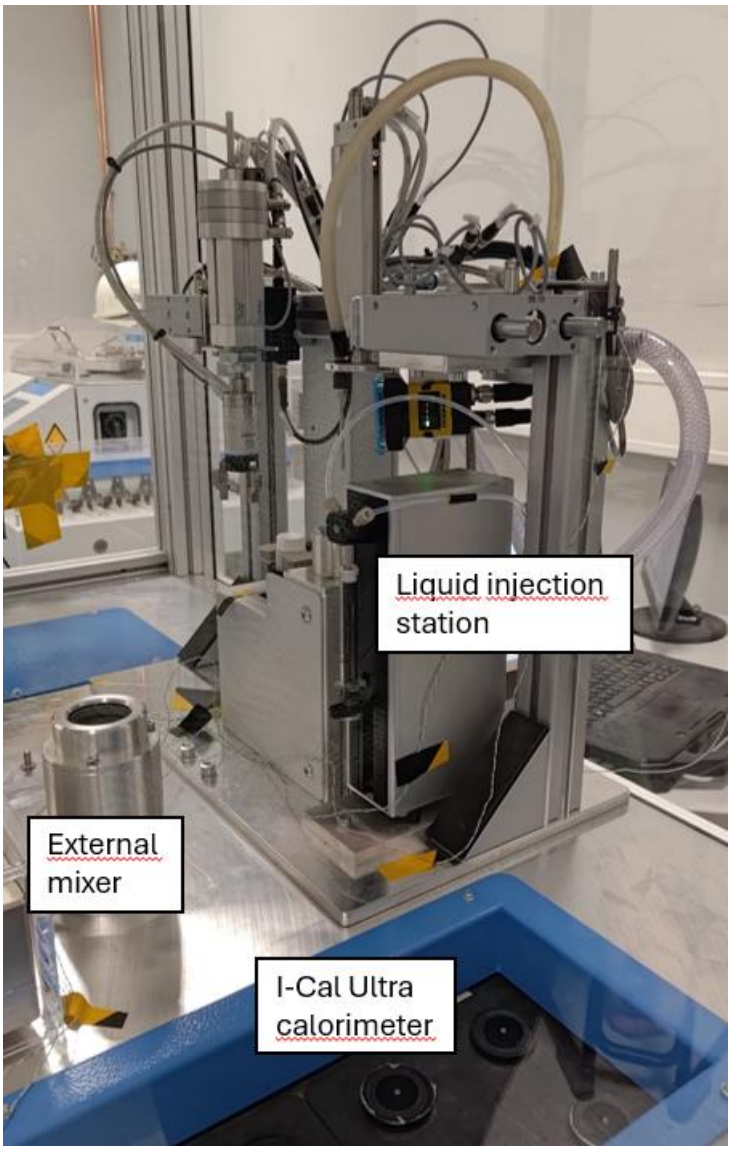

Figure 10. The water injection occurs automatically, based on the weighed sample mass to ensure the right w/s ratio. The sample is then mixed in the ex-situ mixer, before it is placed in the calorimeter.

The data provided by the calorimeter is evaluated automatically by TKIS AQCnet laboratory automation software and kept in a fileserver. Based on the high accuracy and repeatability, it has been shown that variations in the curve shape can be linked to changes in reactivity [10]. This can then be further correlated with chemical, mineralogical and process data to optimize process control.

The robot of the polabCal can load about eighteen samples per hour and provides for the removal and discarding of the sample vial, after the measurement is completed.

4. Methods and materials

4.1. The samples

The nine clinker samples were provided by thyssenkrupp Polysius; three clinker materials with various C_3A content had been ground into powders with three different Blaine numbers (3000, 4000 and 5000 cm^2/g respectively). Mineralogical and chemical analyses are presented in Table 3 and Table 4 respectively. The quality parameters are summarized in Table 5.

Table 3. Mineralogical analysis of the clinker samples.

Sample		**Low-C_3A**	**Medium-C_3A**	**High-C_3A**
Designation	**Unit**			
Alite total	Mass-%	58.3	69.2	60.9
Belite alpha	Mass-%	4.0	1.8	2.5
Belite beta	Mass-%	21.3	9.8	17.3
Belite gamma	Mass-%	-	-	0.3
C_3A cubic	Mass-%	0.7	4.4	9.9
C_3A orthorhombic	Mass-%	0.4	0.2	1.1
C_4AF	Mass-%	13.8	9.9	5.8
Aphthitalite (1)	Mass-%	0.0	0.4	0.2
Arcanite (2)	Mass-%	0.0	1.4	0.7
Lime	Mass-%	1.0	1.4	0.1
Langbeinite (3)	Mass-%	0.0	0.3	0.4
Periclase (4)	Mass-%	0.1	0.8	0.7
Quartz	Mass-%	0.1	0.3	0.1
Portlandite (5)	Mass-%	0.2	0.0	0.2
Sum	**Mass-%**	**100.0**	**100.0**	**100.0**

(1) An alkali sulfate mineral, chemical formula: $(K, Na)_3Na(SO_4)_2$
(2) A potassium sulfate mineral, chemical formula: K_2SO_4
(3) A potassium magnesium sulfate mineral, chemical formula: $K_2Mg_2(SO_4)_3$
(4) A magnesium mineral, chemical formula: MgO
(5) An oxide mineral, chemical formula: $Ca(OH)_2$

Table 4. Chemical analyses of the clinkers.

Sample	**Low-C_3A**	**Medium-C_3A**	**High-C_3A**
Designation			
Mass-% GV	0.48	0.56	0.37
Mass-% SiO_2	23.55	20.93	21.56
Mass-% Al_2O_3	3.94	4.92	6.11
Mass-% TiO_2	0.16	0.23	0.31
Mass-% Fe_2O_3	4.96	2.95	2.73
Mass-% Mn_2O_3	0.07	0.04	0.07
Mass-% CaO	65.17	64.82	64.63
Mass-% MgO	0.76	2.05	1.51
Mass-% SO_3	0.29	1.10	0.89
Mass-% P_2O_5	0.02	0.18	0.12
Mass-% Na_2O	0.09	0.19	0.20
Mass-% K_2O	0.19	0.98	0.77
Mass-% SrO	0.06	0.35	0.30
Mass-**% Sum**	**99.30**	**99.74**	**99.57**
Mass-% CO_2	0.38	0.34	0.29

Table 5. Quality parameters of the clinkers.

Sample	**Low-C_3A**	**Medium-C_3A**	**High-C_3A**
Designation			
LSF	0.48	0.56	0.37
SR	23.55	20.93	21.56
AR	3.94	4.92	6.11

Throughout the rest of the report the three clinker types will be named L, M, and H based on their *low* (L), *medium* (M), and *high* (H) C_3A content, respectively. For differentiation between the various fineness values within the same material, the labels 3K, 4K and 5K have been used, with the numbers representing the degree of grinding, from 3000 to 5000 Blaine. The measured Blaine values are given in Table 6.

Table 6. Overview of the targeted Blaine values of the different clinkers and the actually measured Blaine values, both given in cm^2/g.

Sample	**Low-C_3A**			**Medium-C_3A**			**High-C_3A**		
Targeted Blaine value (cm^2/g)	3000	4000	5000	3000	4000	5000	3000	4000	5000
Measured Blaine value (cm^2/g)	2950	3960	5080	3050	4050	5260	2950	3930	5020

The measurements performed at the manually managed stand-alone I-Cal Ultra allowed the injection of aqueous solutions with varying sulfate content, while in the present polabCal there was only one source of liquid pure water.

Apart from different sample compositions, there were also differences in other parameters, such as sample weight and analysis time. For this reason, the method description has been further divided into two different sections, where the manual and automated experiments are depicted in more detail separately.

4.2. Manual measurements with the I-Cal Ultra

For the experiments on the manually treated samples, three different injection liquids were initially prepared – one consisted of pure deionized water and two were aqueous potassium sulfate solutions, K_2SO_4 (aq). The latter were made in two different concentrations – one providing 1 % and the other 2 % SO_3 in regard to the clinker mass.

The combination of three C_3A contents, three different Blaine numbers, and three possible sulfate concentrations gave rise to 27 unique samples. The samples were labelled based on the three variables, so, for example, 'L–3K–0%' denoted the sample with lowest C_3A content of the lowest Blaine and with no additional sulfate in the injected water.

Towards the end of the project, two further injection liquids with 0 % and 1 % SO_3, but also with an added superplasticizer (MAPEI's Dynamon NRG-700 with a concentration of 1 mass-% in regard to the clinker) were used.

When performing the calorimetric measurements, 3 g of cement clinker were placed in the ampoule and two of the three syringes were loaded with 0.75 mL of injection liquid each (i.e. 1.5 mL in total) to achieve a water/solid ratio of 0.5. The weighing of the clinker was made on a calibrated balance with an accuracy of 0.2 % (i.e., within the range of 2.994 and 3.006 g), which was more precise than the calibration coefficient. The water injection was initially also tested on a balance to ensure a correct injection volume.

After loading, the samples were allowed to reach a thermal equilibrium, i.e., a constant value (baseline). The in-situ injection was then carried out during 5 seconds under stirring and followed by 15 seconds of only stirring, as illustrated in Fig 11. The mixer was rotating at a speed of 133 rpm.

The measurements were run for 24 h, with only some exceptions, and repeated at least three times.

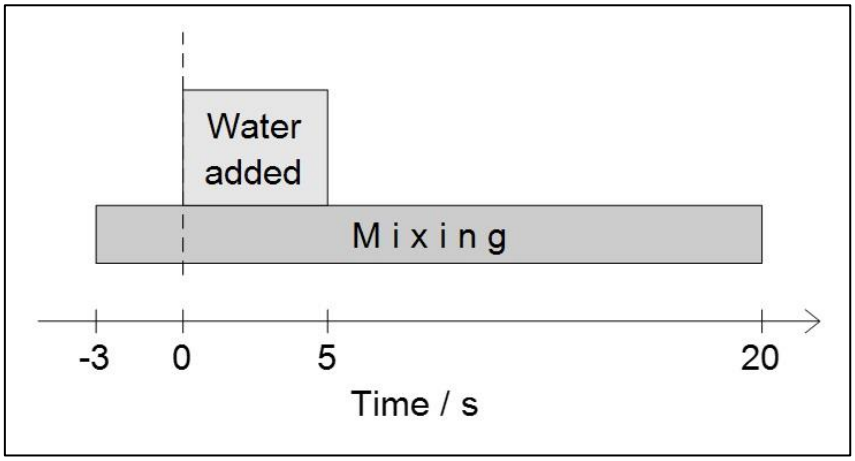

Figure 11. A time scheme of the in-situ injection and mixing procedure.

Prior to performing measurements on the clinker samples, the method was tested on a commercial cement.

Calibration coefficients were determined by electrical pulse calibration conducted with polyurethane resin encapsuled heaters contained in the same type of vials as were used during the later measurements. During the calibration, a thermal power of about 40 mW was applied per heater –10 min on and 3 h off.

The temperature in the calorimeter was set to 20 °C. Both the baselines and the calibration coefficients were measured four times during the project. The coefficient of variation of the calibration coefficient was determined to be less than 0.5 %.

4.3. Measurements with the polabCal

There were three different types of automated experiments carried out; in a first step, the same pure clinker samples were used as in the manual measurements and in a second step, measurements were made on mixed clinker samples, as shown in Table 7. Thirdly, all clinker samples were run for 24 h (1440 min) with the same setting parameters.

The target value for the mass was 5.00 g and the w/s ratio to 0.50. The thermostating time was set to 20 min and, for the first two steps, the analysis time to 90 min. All the water injected was pure, i.e., without any added sulfate. The calorimeter was operating at 20 °C.

Table 7. Summary of the measurements conducted on mixed clinkers with different C_3A content. Equal masses (2.5 g) of each clinker were used in the mixes.

Clinker	Blaine
L + M	3000
L + M	4000
L + M	5000
M + H	3000
M + H	4000
M + H	5000

4.4. Data analysis

All the data files were transferred into MATLAB and evaluated in programs specially developed for this project. These were adjusted in diverse ways to, for example, gather the graphs from certain samples and, thereby, easily be able to compare results and look for trends regarding the three variables C_3A content, Blaine number, and sulfate content.

For the data analysis, the mixing quality was also assessed and graded according to its visually appearing homogeneity and morphology of the hardened sample. The idea was

to exclude poorly mixed and, hence, insufficiently hydrated samples from the data evaluation.

To define the true thermal power produced during the hydration process based on the measured thermal power, a thermal lag (Tian) correction was used, as described in the section *3.1.3 Calibration and calculations*.

5. Results and discussion

As outlined in *1.1 Aim*, there were three main focus areas in this project.

Due to the substantial number of successfully performed measurements and to the many different possibilities of interpreting the results of these, not all of the graphs are reproduced here. Instead, this section is based on the goal of answering the three main research questions.

For the analyses, the indices shown in Fig 12 were used. Please note that these apply to the Tian corrected curves and that all calorimetric power-time curves presented in *5. Results and discussion* have been Tian corrected, unless otherwise specified. The notations P_1 and P_2 define the maximal thermal power generated during the early (0–20 min) and main (20 min–24 h) reactions respectively. Q_1 and Q_2 are the corresponding integrals of P_1 and P_2, calculated according to Equation (7) in the section about *3.1.3 Calibration and calculations*. Mathematically expressed and with the time t given in minutes,

$$Q_1 = \int_{t=0}^{20} P_1 \, dt \quad \text{and} \quad Q_2 = \int_{t=20}^{1440} P_2 \, dt. \tag{8}$$

However, two complications were found regarding the use of Q_2 – firstly, not all measurements lasted for 24 h and secondly, some retarded samples did not exhibit any peak within the first 24 h. For this reason, Q_1 was mainly used for interpreting the results.

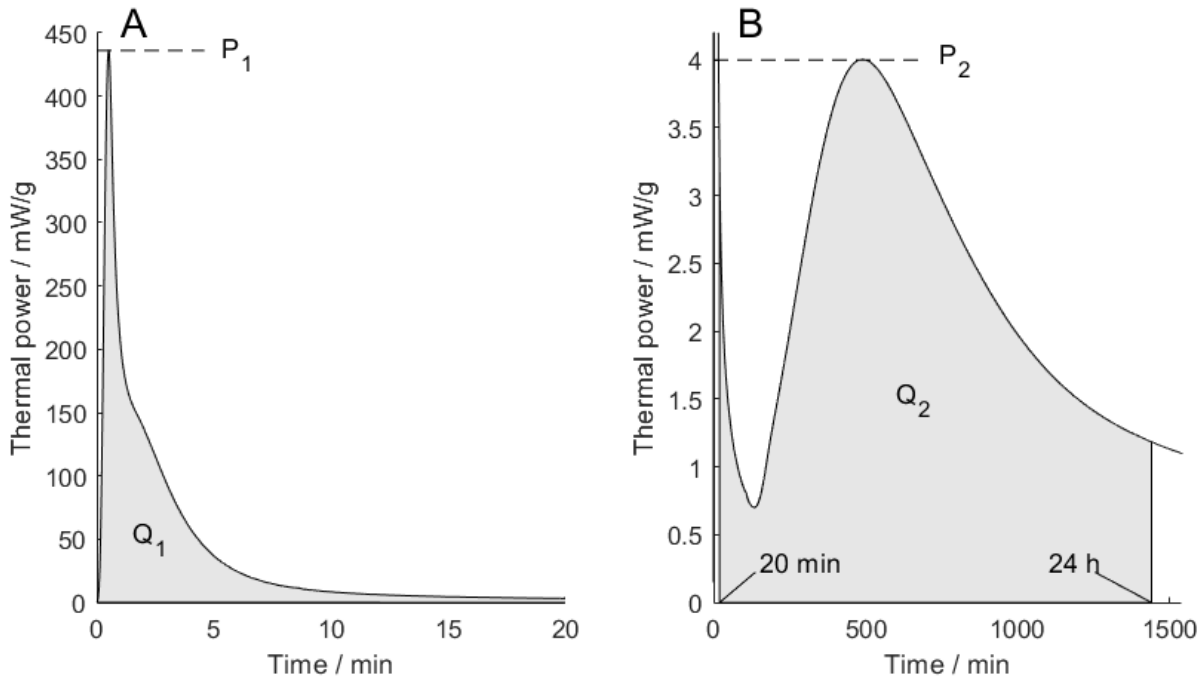

Figure 12. Illustration of the indices used in the data analyses. P_1 denotes the thermal power of the early reaction peak and P_2 is the equivalent for the main reaction. Q_1 and Q_2 represent the integrated thermal power (i.e., the overall heat) of the early reaction peak and the main reaction peak respectively.

5.1. Differences between in-situ and ex-situ mixing

The most direct and obvious difference observed when comparing the results of the in-situ and ex-situ mixing respectively was the mixing quality. Difficulties were expected to arise when mixing the high-C_3A–high-Blaine samples due to possible flash setting, and these samples were also hard to mix properly with the in-situ mixer. However, also other samples exhibited different mixing issues with the in-situ mixer but, most notably, it was hard to see any clear patterns, as there was no consistency regarding the mixing quality and visual morphology of the hardened samples.

Tests with mixing samples with the mixing vessel outside the calorimeter and with a cut-open vial, showed that in all cases the sample looked like a low-viscosity fluid during the first half of the 15 s mixing, while it in the cases where the morphology of the hydrated samples looked odd, the change in morphology occurred after about half the mixing. This indicates that in the samples with oddly hardened morphology, but no signs of dry clinker, the clinker and the water were macroscopically well mixed.

The samples mixed ex-situ exhibited a significantly higher consistency regarding the mixing quality and this applied to all clinkers and Blaine values.

It was known, already from the start, that the in-situ mixing with a mechanical stirrer would provide a weaker agitation than the intense shaking achieved in the ex-situ mixer. However, it was not expected that the difference would be so significant. This remarkable difference in mixing quality also had an effect on the resulting curves.

5.1.1. Manual measurements with the I-Cal Ultra

As mentioned under *4. Methods and materials*, a commercial cement was initially tested to get a picture of the repeatability and reliability of the instrument and the method. In Fig 13, both the early hydration peak (a), occurring within the first minutes, and the main hydration peak (b), developing over several hours, can be seen. In (a) one can also observe the effect of the thermal inertia of the system, as the dashed lines show the data recorded by the heat flow sensor, while Tian corrected results (solid lines), meant to reproduce and mirror the actual heat generation, exhibit a remarkably higher and more distinctive peak. The mixing quality of the commercial cement was high and even throughout all the samples and, as the graphs exhibited high reproducibility, this indicated that both the method and the instrument were well-functioning.

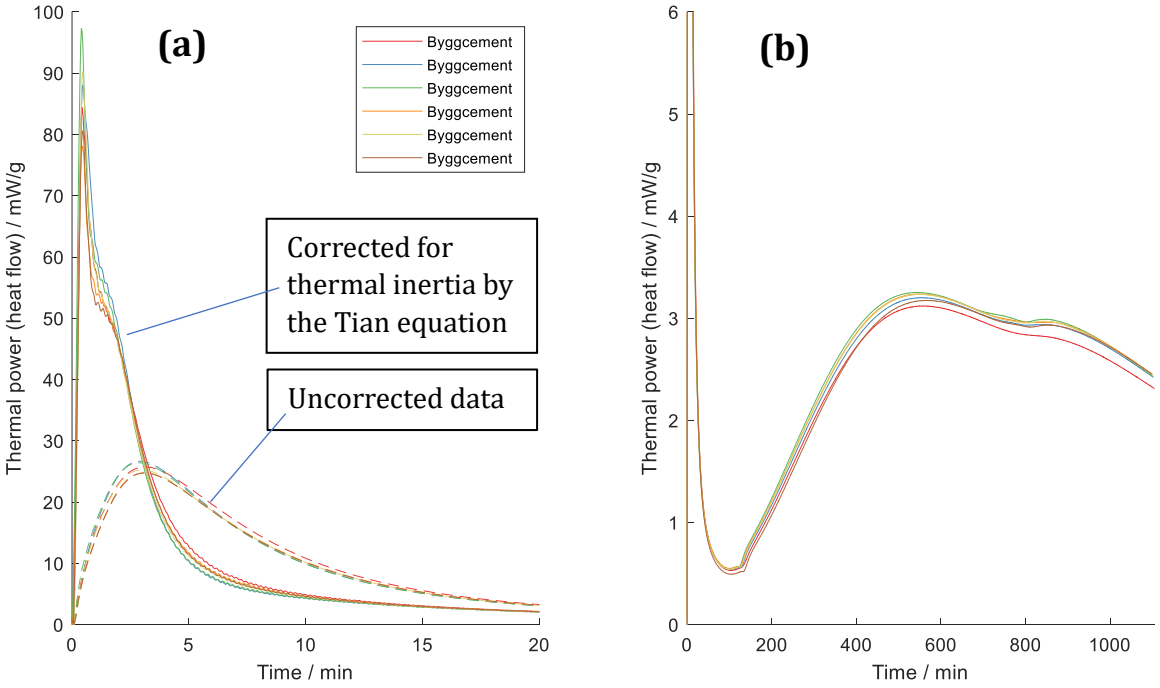

Figure 13. Calorimetric power-time curves generated from measurements on commercial cement. In (a), the first 20 min of hydration are shown with the dashed lines showing the measured heat flow and the solid lines representing the Tian corrected heat flow. In (b), 18 h measurements are shown. It is worth noting the substantial difference in peak height between the first and the second peak (about 90 and 3 mW respectively).

The challenges appeared when the cement clinker measurements were initiated. The photographs in Fig 14 display some samples, exhibiting large variations in the mixing and morphology of the hardened material.

As already mentioned under *4.4 Data analysis*, the calorimetric data generated from the well and intermediately mixed samples were further used for evaluation, while samples containing a substantial amount of obviously unhydrated material, were excluded from further interpretation.

Figure 14. Examples of different mixing qualities achieved through in-situ mixing. To the left are examples of the most homogeneous samples, while the sample to the right was very poorly mixed and not homogeneously hydrated. The middle picture shows intermediate mixing quality, for which it was assumed that the samples were sufficiently hydrated.

5.1.2. Measurements with the polabCal

The automated measurements were fewer and partly shorter than the manual ones (the manual measurements mostly extended over 24 h, while a big part of the automated measurements were carried out during only 90 min). However, as the results from the automated measurements were more reproducible and since the first hydration peak was an important part of the thesis work (see *1.1 Aim*), the generated results provided sufficient material to observe patterns and draw certain conclusions.

As described under *4.3 Measurements with the polabCal*, automated measurements were conducted on samples with mixed clinkers. The resulting curves can be seen in Fig 18 under *5.2.1 The influence of the C_3A content* and are further discussed there.

5.1.3. Comparison of calorimetric results

When comparing the data and the corresponding graphs resulting from the manual and automatic measurements, respectively, there are some things worth noting. In Fig 15, the results from all the clinkers with Blaine 4000 and 0 % SO_3 are presented. The figures are arranged with increasing C_3A content from top to bottom with the graphs on the left side showing the initial peaks within the 20 first min of hydration and the right-hand plots showing measurements during 24 h. As the automated measurements did not have any additional SO_3 in the injection water, only the manual measurements with 0 % of added SO_3 are plotted here.

The curves of the automated measurements (blue lines) appear with a certain delay in relation to the curves of the manual measurements (orange lines). Time zero in the plot is the time of the water injection. However, as the robot doing the automated measurements needed approximately 75 s to transfer the ampoule from the water injection station to the mixing station and further down into the calorimeter, this caused a postponement of the start of the calorimetric measurements.

The blue graphs also display a much lower P_1, while the main reactions tend to accelerate sooner. The latter observation is most likely a consequence of the more efficient mixing. The efficiency of the mixer can supposedly also explain the significantly higher reproducibility of the automated measurements.

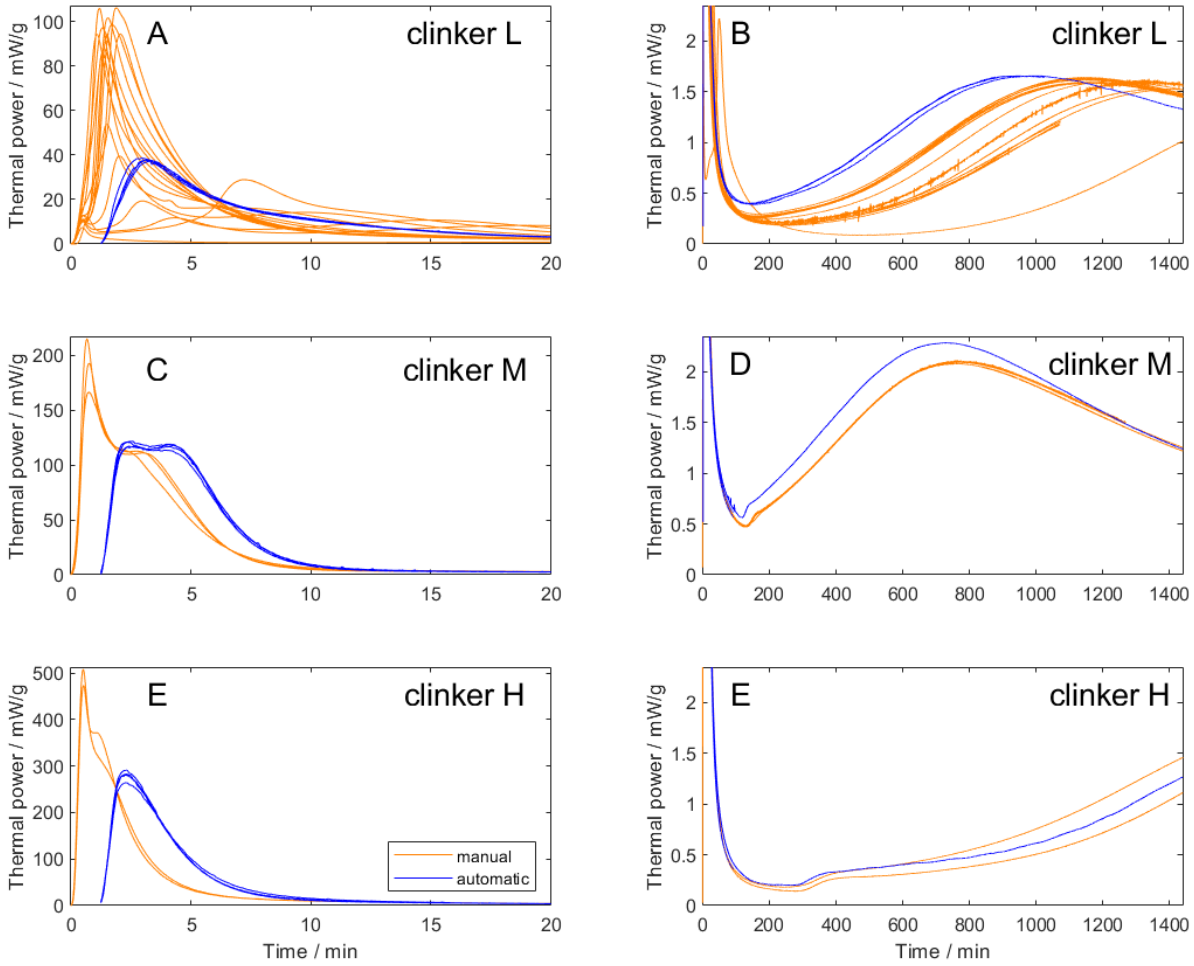

Figure 15. Comparison of the manually (orange lines) and automatically (blue lines) conducted measurements on all the clinkers with Blaine 4000 and no additional SO_3. In A, C and E the first 20 min of hydration are shown; B, D and E show the results from 24 h. Please note the different scaling on the y-axes of A, C and E.

It is worth noting that the scale on the y-axes in Fig 15 vary markedly between the different clinkers for the early reactions, with P_1 values reaching between about 100 and 500 mW/g, while the development of the thermal power is more uniform for the main reaction. In the case of clinker H, the main reaction is greatly retarded – a possible indication of flash setting.

The early reaction of clinker M proceeded for a longer period of time compared with clinker H. There is also a double peak appearing in the early reaction stage of clinker M. This could possibly be explained by the fact that clinker M was the one, among these

clinkers, that came with the highest amount of SO_3 included in the raw material (see Table 3 under *4.1 The samples*). Consequently, even though no SO_3 was added to the injection liquid of these samples, for the M samples, there might have been sufficient soluble SO_3 amounts available for C_3A to first react with water under the formation of ettringite, before the system ran out of SO_3 and the reaction switched to the production of calcium aluminate hydrates, as described in *2.3.1 Hydration products*. Such a shift in reaction can appear as a double peak.

The overall heat of reaction, $Q = Q_1 + Q_2$, was also analyzed and the graphs of $Q(t)$ are presented in Fig 16, where it shows that Q_1 increased with the C_3A content.

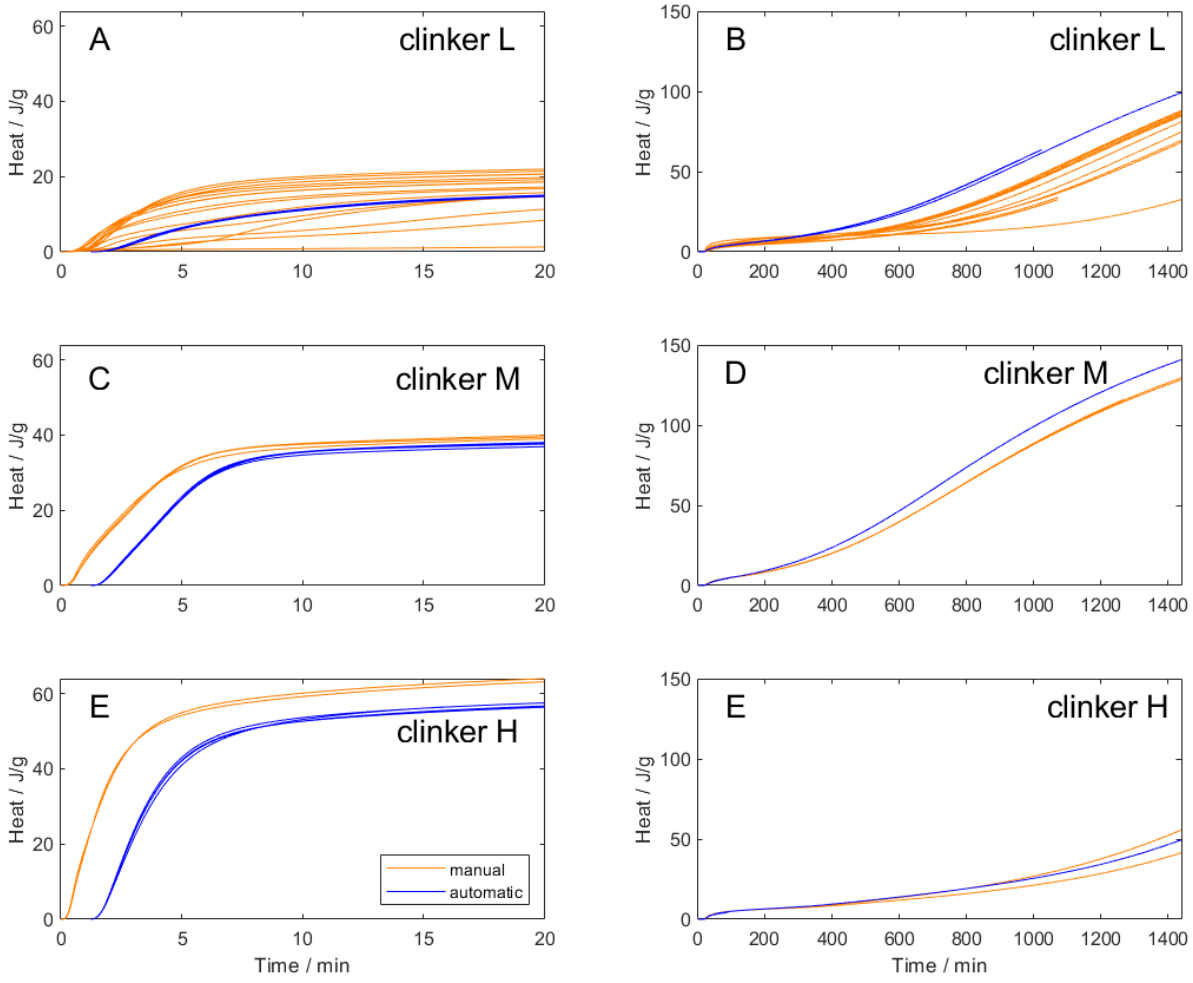

Figure 16. Comparison of the overall heat Q(t) for the manual and automated measurements on all clinkers with Blaine 4000 and 0 % added SO_3. In B, D and E, the integration was started at 20 min, so that A+B, C+D and E+F respectively together give all the heat up to 24 h.

There is a very large spread in results of the manual measurements for clinker L with no SO_3, both when it comes to thermal power and overall heat of reaction. As the graphs from the automated measurements do not exhibit the same spread, the most probable is a connection to the differences in the mixing.

For the clinkers M and H, the integrated thermal power of the first 20 min of hydration, Q_1, was clearly lower in the automated measurements. This could be due to heat loss on the way from the injection station to the calorimeter.

Clinker H generated the largest Q_1 value. This was expected, as C_3A reacts rapidly with a considerable heat release. Nevertheless, clinker M was the one with the highest integrated thermal power of hydration between 20 min and 24 h, Q_2. This can be linked to the strong retardation of clinker H seen in Fig 15, which hindered it from reaching higher values of Q.

To see, if there was any general correlation between the peak height P_1 and the integrated heat Q_1, a plot of these was made for all the measurements. The result in Fig 17 shows a relatively good correlation between the two parameters, meaning, for example, that a high P_1 can be associated with a high Q_1.

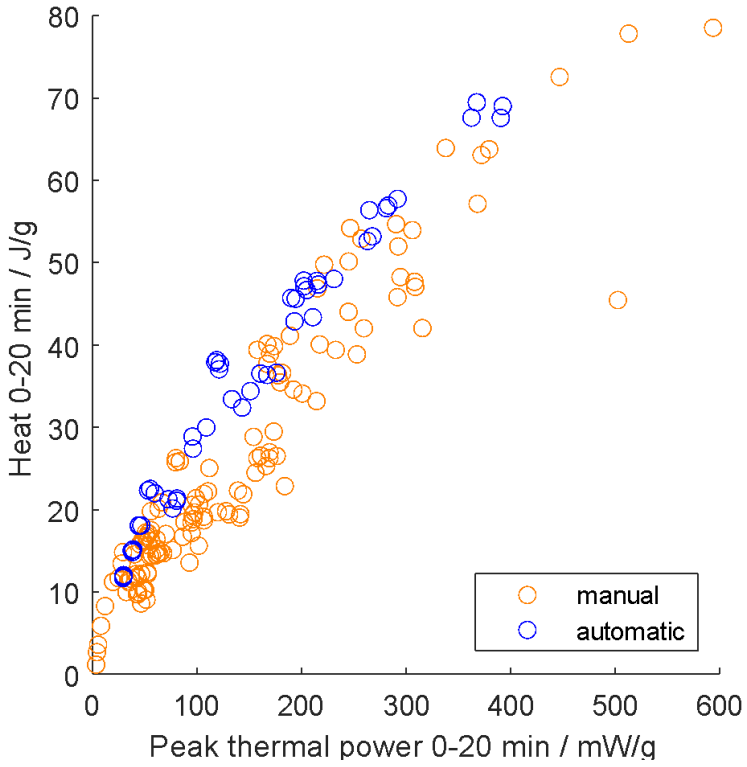

Figure 17. The integrated thermal power of the first 20 min of hydration, Q_1, plotted against the thermal power of the early reaction peak, P_1, for all measurements.

The reason that the automated data lies above the data from the manually treated samples, is that the automated results in general have slightly lower Q_1, but a much lower P_1. This means that the manual and automatic markers close together in the plot do not represent the same samples and one should thus not compare these to each other.

5.2. Linking the early calorimetric results to chemical processes

To better understand the connection between the development of thermal power and the reactions taking place within the sample, the impact of the three variables C_3A content, Blaine number, and SO_3 concentration in the injection water was evaluated. This has partly been discussed already in the above section but will now be outlined a bit further.

5.2.1. Influence of C_3A content

As already mentioned, the presence of C_3A contributed to a rapid increase in the early reaction rate with a corresponding heat development; in Fig 15, there is a clear trend towards a higher P_1 with an increase in C_3A content and, in accordance with the correlation shown in Fig 17, this also generated the highest integrated heat of the early reactions, Q_1 (Fig 16).

For the main reaction, it can be seen that the higher levels of C_3A required more SO_3 in solution to control the reaction and avoid flash setting. The retarded main reactions of clinker H which appear in Fig 15 is an evident result of SO_3 deficiency in the system.

During the laboratory work, it was difficult to achieve a sufficiently good in-situ mixing of the samples with high Blaine and low (or zero) SO_3 concentrations, which unfortunately resulted in plenty of measurements being excluded from further analysis. The ex-situ mixer, however, managed to overcome these problems.

The automated measurements that were carried out on mixed clinker samples intended to investigate the effect of creating intermediate C_3A levels to overlap the gaps between the different clinkers. As shown in Fig 18, mixing the clinkers L and M generated curves that were not in between the two unmixed clinkers, which was the case when mixing the clinkers M and H. There was, obviously, complex chemistry involved that not only included the containment of C_3A, but also interaction with other phases. This will, however, not be further analyzed here.

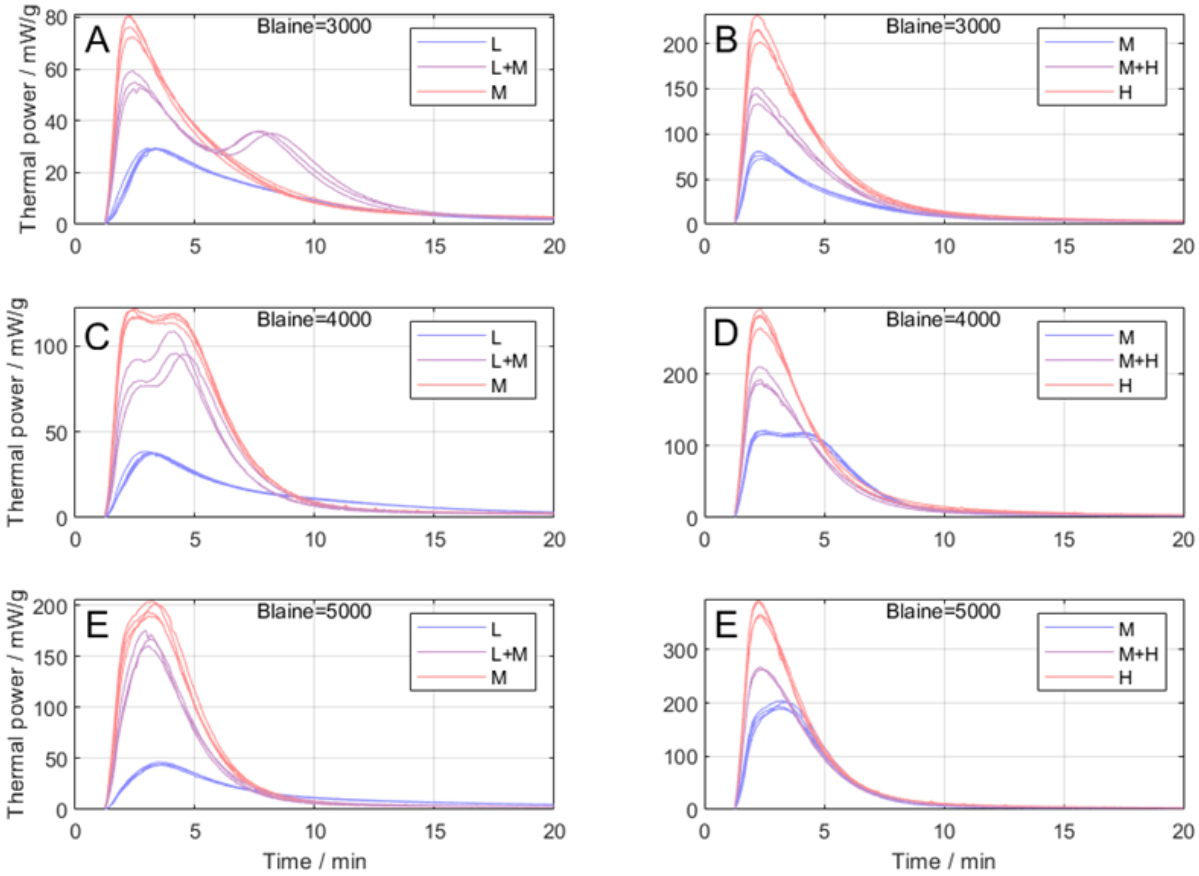

Figure 18. Calorimetric power-time curves resulting from measuring the hydration of mixed clinkers. Clinker M is present in both mixtures, L+M and M+H respectively; its thermal power is represented by a red line on the left side and a blue line on the right side. Please also note the different scaling on the y-axes.

5.2.2. Influence of Blaine number

As the data generated from the automated measurements exhibited a higher reproducibility and gave rise to more distinctive curves, these were used when evaluating the impact of the Blaine number on the appearance of the calorimetric power-time curves. The power-time curves in Fig 19 show a clear trend for the different Blaine values, both in the early and main reactions; the higher the Blaine value, the higher is also P_1, and the earlier does the main reaction occur.

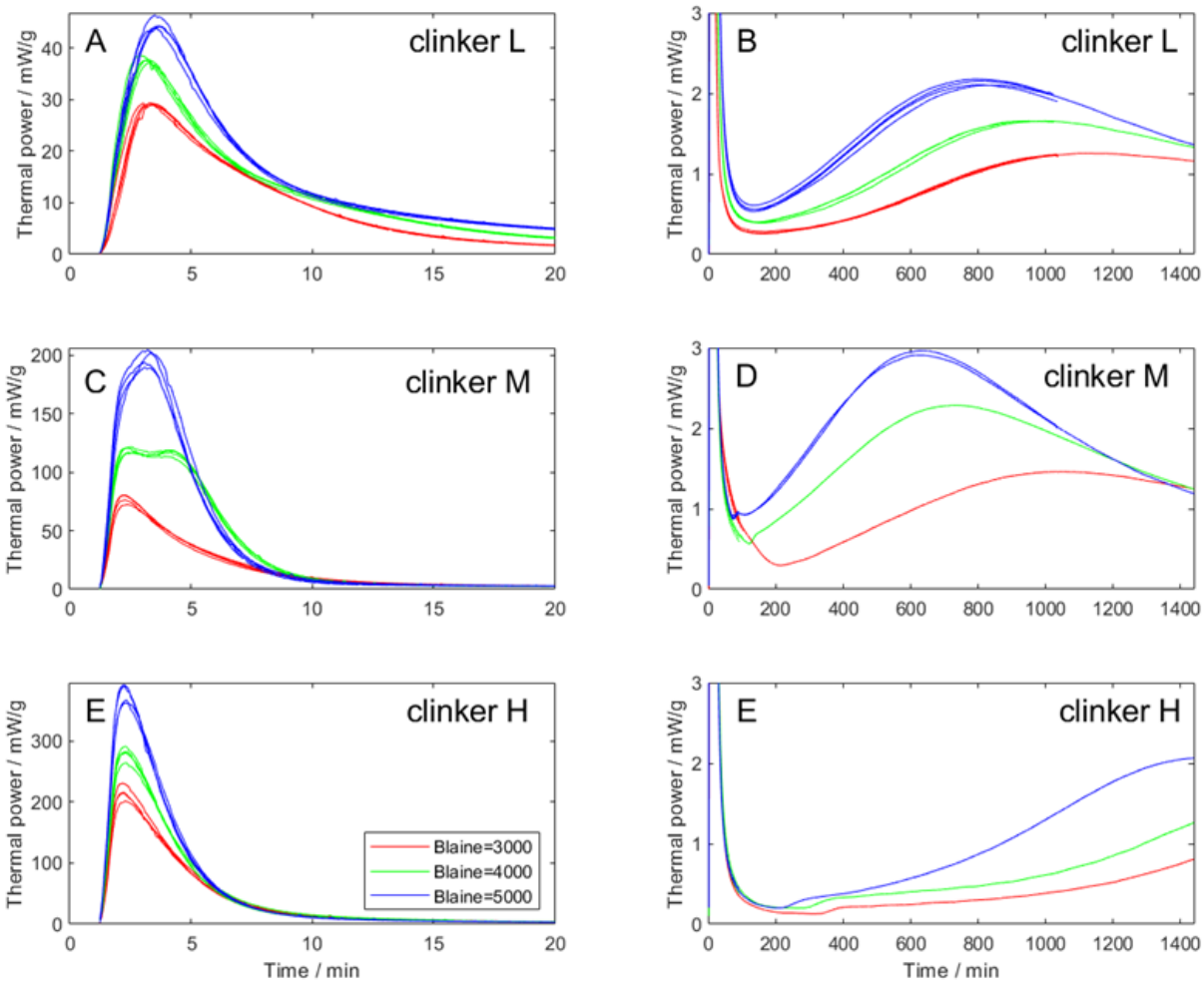

Figure 19. Calorimetric power-time curves generated from the polabCal measurements, i.e., with no additional SO_3. One can observe a clear retardation of the main reaction for clinker H. Higher Blaine values gave rise to higher thermal power and an earlier main reaction. In A, C and E the first 20 min of hydration are shown; B, D and E show the results from 24 h. Please note the different scaling on the y-axes of A, C and E.

These results seem reasonable, as the larger surface-to-volume ratio that comes with an increasing Blaine number enables more anhydrous material to dissolve per time unit, which in turn speeds up the hydration process and leads to an increased heat production.

Compared to the corresponding manual results seen below in the subplots A and B of Fig 20, Fig 21, and Fig 22 respectively, the peaks are higher here, both for the early reaction and for the main reaction.

5.2.3. Influence of SO_3 content in solution

There was a clear positive effect on the results observed for all the clinkers with an addition of SO_3 into the injection liquid. Please note, that the results discussed in this section were retrieved solely from manual measurements, since the automated experiments were conducted only with pure water.

The resulting power-time curves from all clinkers and all Blaine numbers with 0 %, 1 % and 2 % SO_3 are presented in Fig 20, Fig 21, and Fig 22 respectively.

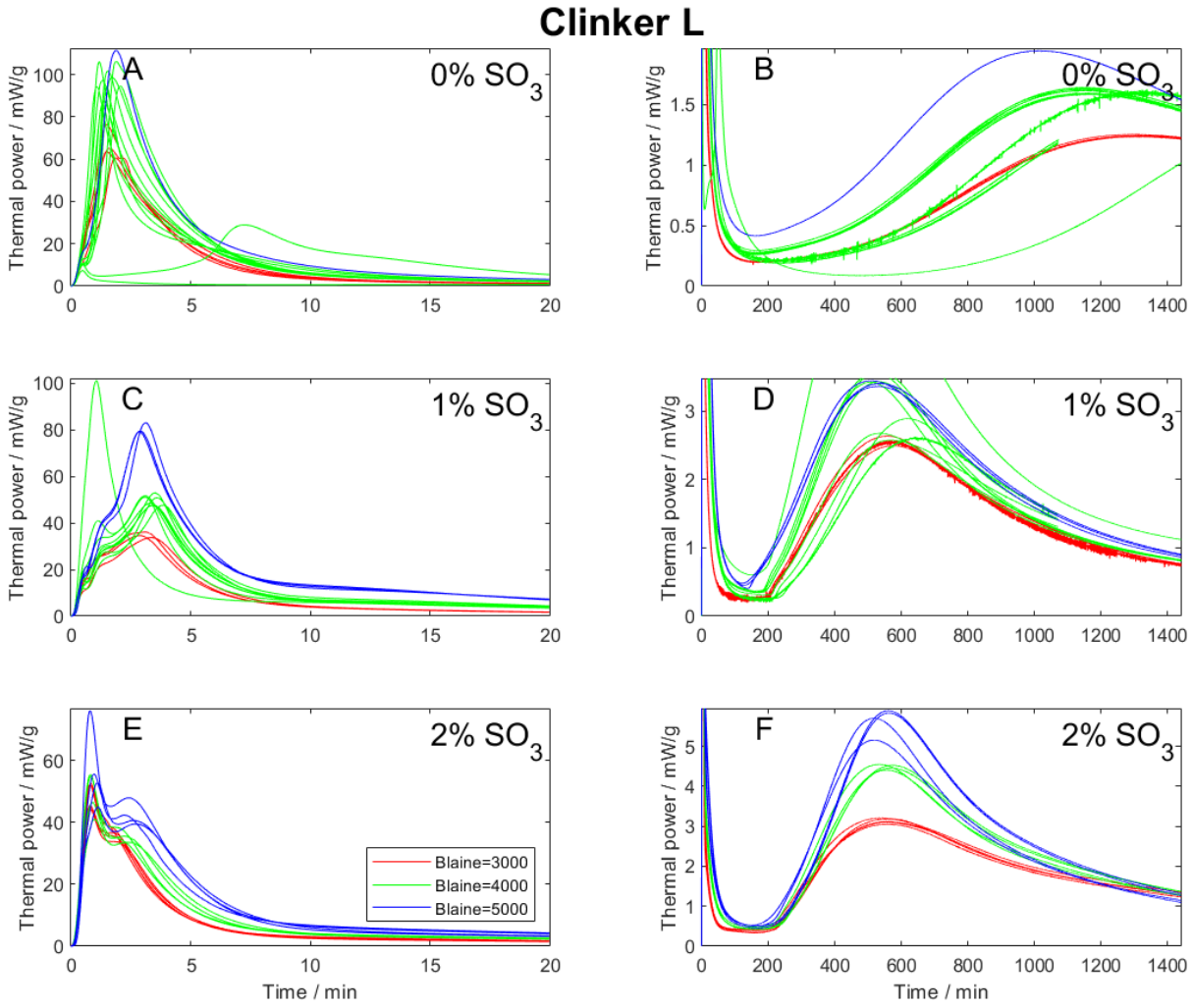

Figure 20. Calorimetric power-time curves for all the Blaine numbers of clinker L and an increasing SO_3 content from top to bottom. In A, C and E the first 20 min of hydration are shown; B, D and E show the results from 24 h. Please note the different scaling on the y-axes.

Clinker L exhibited a large spread among the curves in the subplots A and B of Fig 20, i.e., in the measurements with 0 % SO_3 added. Addition of SO_3 reduced the wide spread of the curves and made the measurements more reproducible. Going from 0 % to 1 % SO_3 collected the results within the same Blaine value, while having a clear distinction

between the thermal power of the different Blaine numbers (except for one odd green curve in Fig 20, subplot B).

Adding 2 % SO_3 further reduced the difference among the Blaine numbers; the different colored early curves came closer together. This pattern can, however, not be seen in the main peak. With 2 % SO_3, the results of clinker L also included an early double peak (Fig 20, subplot E). This is most clearly seen in the blue power-time curve, which falls after the first peak and then rises to pass through another local maximum before gradually falling again. It could be an indication that false setting occurred here, as there was probably excess SO_3 present in the pore fluid.

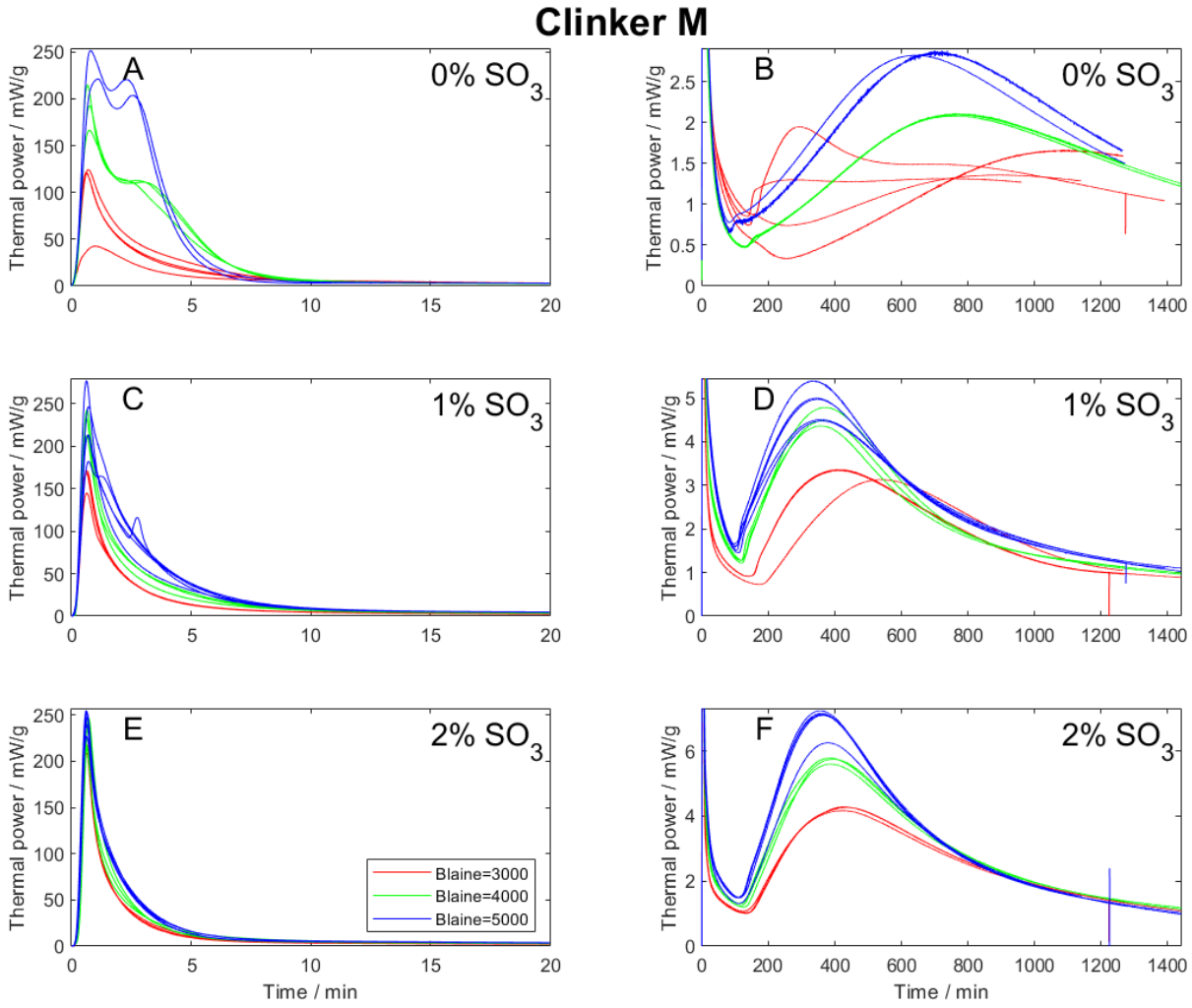

Figure 21. Calorimetric power-time curves for all the Blaine numbers of clinker M and an increasing SO_3 content from top to bottom. In A, C and E the first 20 min of hydration are shown; B, D and E show the results from 24 h. Please note the different scaling on the y-axes.

In subplot A of Fig 21, the results of the high-Blaine clinker M (blue lines) also exhibit a double peak, while the intermediate-Blaine sample (green lines) has a shoulder, a terrace point, on the right side of the initial peak.

With 1 % SO_3 added to the solution, the double peak of the high-Blaine samples became less prominent, the shoulder of the intermediate-Blaine samples disappeared, and the power-time curves of the samples with different Blaine numbers came closer together. Increasing the concentration to 2 % SO_3, made the curves almost overlap.

Adding SO_3 obviously lead to a partial elimination of the impact of different Blaine numbers and, thereby, of the difference in total SSA. It seems that the increase in dissolution rate, and the corresponding heat release, that should come with a higher SSA was not as prominent as expected with dissolved SO_3 present in the liquid.

The change from early double peaks to single peaks indicates, that the early reactions were directed towards ettringite formation. Also, the main hydration peaks of clinker M developed a more assembled and predictable pattern with increasing SO_3 content.

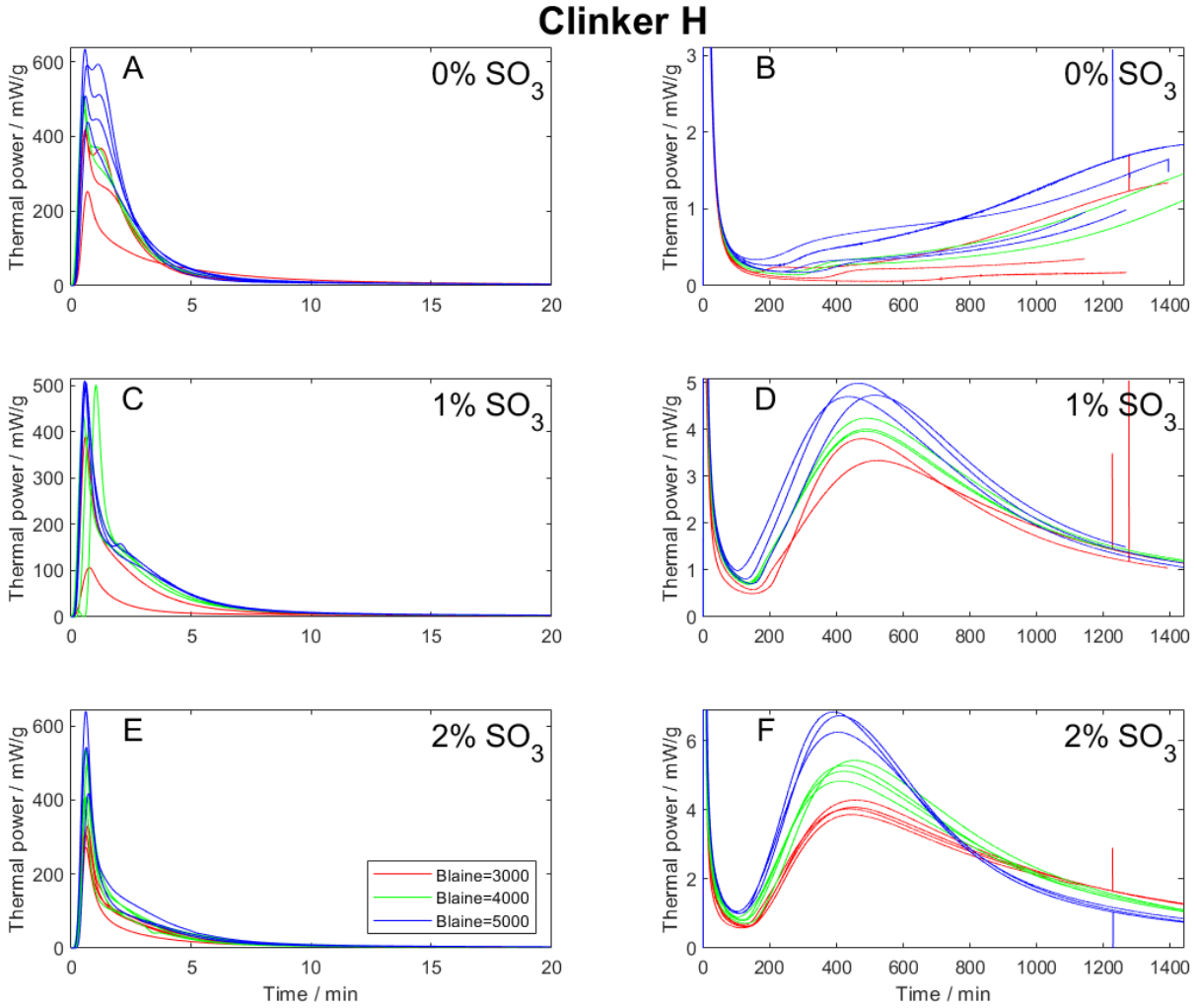

Figure 22. Calorimetric power-time curves for all the Blaine numbers of clinker M and an increasing SO_3 content from top to bottom. In A, C and E the first 20 min of hydration are shown; B, D and E show the results from 24 h. Please note the different scaling on the y-axes.

Clinker H, just like clinker M, displayed double peaks in the early reactions with 0 % SO_3 (Fig 22, subplot A). These disappeared gradually as SO_3 was added to the injection liquid (Fig 22, subplot B and C). The first peak was sharpened and, also here, the curves of the different Blaine-numbers came closer together. For the main reaction there was a crucial difference between 0 % and 1 % SO_3 (Fig 22, subplot B and D), namely the avoidance of flash setting that resulted from the SO_3 addition. The more SO_3, the less retarded was the main reaction – in fact, when going from 1 % to 2 % the main peak appeared earlier.

For all the clinkers, increasing the SO_3 concentration from 0 % to 2 % caused a gradual decrease in P_1 and a simultaneous growth of the P_2 values. This can probably be linked to less formation of calcium aluminate hydrates in the early-reaction stage and prevention of flash setting, providing a more controlled reaction process.

Fig 23 and Fig 24 provide an overview of how the SO_3 concentration influenced the P_1 and Q_1 values of all the clinkers with their different Blaine numbers. The corresponding graphs of P_2 and Q_2 contain errors, due to deficient results in the measurements with 0 % SO_3. These have therefore been deliberately omitted.

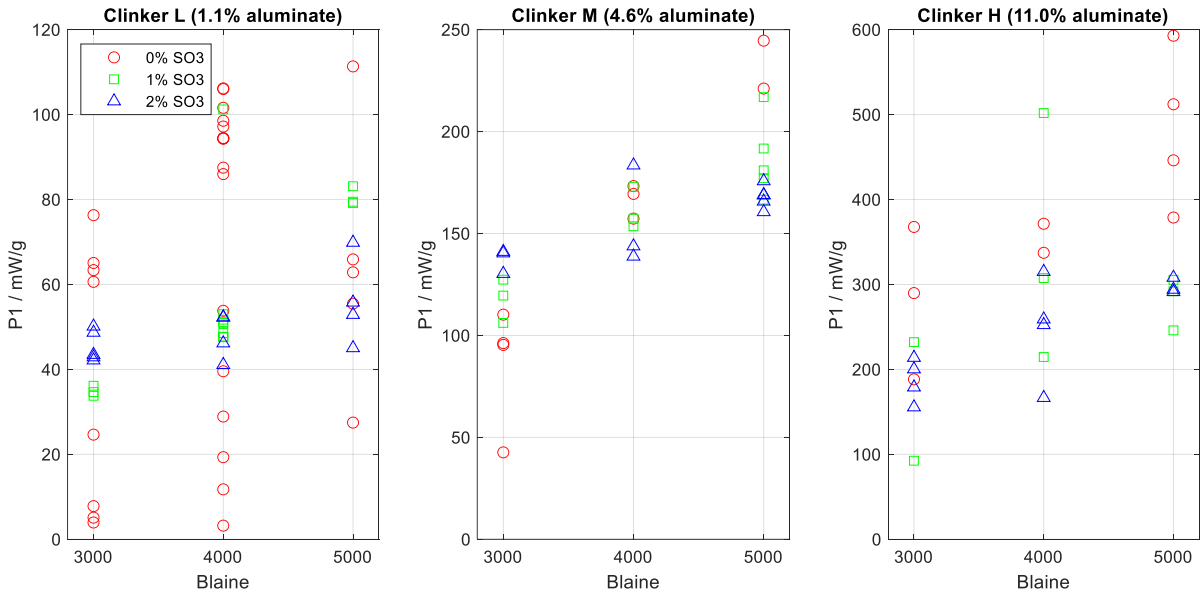

Figure 23. An overview of P_1 for the different clinkers and how it is influenced by the presence of SO_3.

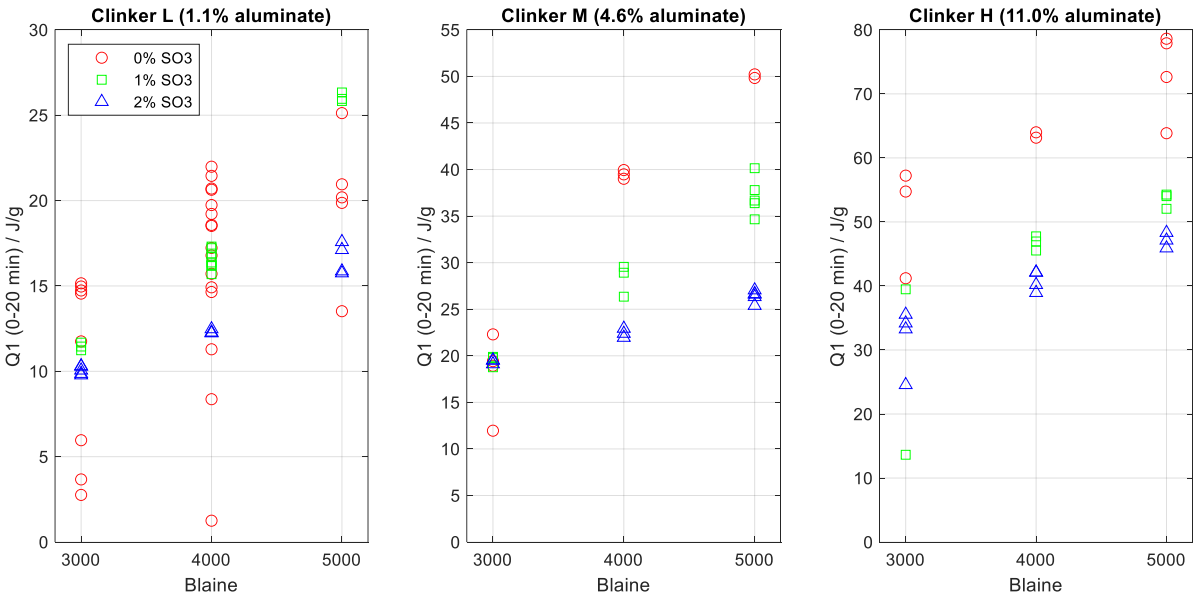

Figure 24. An overview of Q_1 for the different clinkers and how it is influenced by the presence of SO_3.

5.3. Connections between the early and main reactions

As recently shown in the above section (Fig 20, Fig 21, and Fig 22), SO_3 addition had a clear effect on the heat development of the early and main hydration steps. Scattered results in the early reactions also gave large variations in the main peak. In particular, this was important for clinker H which, with its 11 mass-% of C_3A, evidently required the access of dissolved SO_3 to control the hydration; SO_3 deficiency in the beginning lead to the formation of calcium aluminate hydrates which retarded the main hydration peak. This appeared as a flatter curve and indicated a lack of strength development.

It was also shown that the decrease in P_1 resulting from SO_3 addition came with an increase in P_2. One could maybe say that the reactivity of the clinker was dampened in the early reactions and then transferred to the main-reaction stage, thus being leveled out. Further research is however needed to better understand the underlying chemistry and to draw conclusions concerning other parameters, such as the development of compressive strength.

The automatic measurements showed that an increase in the Blaine value was linked to a higher thermal power in the initial peak, P_1, and an earlier start-up of the main hydration.

5.4. Sources of error

Mass of the clinker sample

When it comes to the potential errors in thermal power measurements, the mass of the available clinker is crucial, but it was determined to 0.2 % in all experiments.

Amount of injected water

As mentioned already, the syringes were checked by weighing prior to the measurements to assure the right amount of water being injected into the samples. The water mass dosing was made by visual observations of the water level in the syringes. 95 % of all injections were within an 4 % of the mean value (0.735). As the w/s ratio was already quite high (0.5) this deviation should not significantly have impacted the hydration.

Mixing

The mixing of the samples was in focus throughout the whole project, and it was known, already from the beginning, that the in-situ mixing could be insufficient for at least some of the samples. The possibly negative effects of this were considered both during the laboratory work and in the data analysis by excluding measurements of the samples that were obviously poorly mixed (see *4. Methods and materials*). Nevertheless, it was not possible to evaluate the errors emerging from insufficient mixing.

Materials

The clinker powders are extremely homogeneous but also highly hygroscopic, meaning that inappropriate storage can cause the clinker to prehydrate and change its reactivity. For this reason, the clinker samples were stored in sealed containers with a drying agent. The potentially modified reactivity of the clinker samples over time (about three months) was, however, not studied explicitly and it is therefore not possible to assess the impact of this on the overall results.

5.5. Suggestions for future studies

Samples of mixed clinkers were analyzed in automated experiments. Due to time limitations, it was however not possible to also perform measurements on samples with mixed Blaine values. It would be interesting to combine samples of the same clinker but different Blaine, as shown in Table 8. The idea would be to create a two-dimensional matrix of results with gradually changing C_3A content in one direction and gradually changing proportions of different Blaine numbers along the other. Based on this, one could maybe gain further understanding of clinker hydration processes and the interaction between these.

Table 8. Suggestion on how, in future studies, different Blaine numbers could be mixed within the same clinker type.

Clinker	Blaine
26	3000 + 4000
26	4000 + 5000
09	3000 + 4000
09	4000 + 5000
96	3000 + 4000
96	4000 + 5000

Furthermore, it would be interesting to intergrind the clinker with SO_3 (which essentially means to form cement) and to examine the impact of various amounts of different sulfate carriers.

To find out more about the chemical processes taking place, the calorimetric experiments could be complemented with analyses from ion-selective electrodes and perhaps also conductivity measurements to closer investigate processes of, for instance, dissolution and precipitation.

Thermodynamic calculations including enthalpies of both reactants and products could also be considered in future work, to complement different types of analyses and, for example, fill in the gaps that exist regarding amorphous materials which cannot be studied by means such as XRD/XRF.

6. Conclusion

Referring back to *1.1 Aim* and the three main focus areas of this project, the following can be concluded.

1) The results of the calorimetric measurements exhibited differences, depending on the mixing type used. In-situ mixing resulted in significantly poorer mixing quality on a visual level, and a more scattered and unpredictable development of the thermal power. The ex-situ mixer of the polabCal provided much more consistent and repeatable mixing and calorimetric results, even though there was no additional sulfate added to the injection liquid. The better mixing achieved in the polabCal also lead to higher initial peaks and an earlier onset of the main reaction. However, there was the disadvantage of losing the first minutes' kinetics (and possibly also heat) due to the time required to insert the vial into the calorimeter.

2) A higher C_3A content led to a more rapidly increasing early hydration curve, a higher initial peak, and an elevated total heat of the early reactions. It was also shown that the clinker with the highest C_3A content (about 11 mass-%) required additional SO_3 to avoid flash setting.
   Increasing the SO_3 concentration from 0 % to 2 % caused a gradual lowering of the early hydration peak and a simultaneous rise in the peak of the main hydration, for all the clinkers. The addition of SO_3 also led to more consistent results and gave rise to curves of different Blaine numbers coming closer together. The early double peaks displayed by the two clinkers with the highest C_3A contents with no added SO_3 were replaced by a single peak when SO_3 was provided through the injection liquid.

3) For all clinkers it was shown that scattered results in the early reactions were associated with large variations in the main hydration. A higher Blaine value was linked to a higher thermal power in the initial peak and an earlier onset of the main hydration.

References

[1] W. D. Callister, Jr. and D. G. Rethwisch, Callister's Materials Science and Engineering, Asia: Wiley, 2020.

[2] W. Kurdowski, Cement and Concrete Chemistry, Springer, 2014.

[3] H. Taylor, Cement Chemistry, London: Thomas Telford Publishing, 1997.

[4] C. E. Housecroft and A. G. Sharpe, Inorganic Chemistry, Harlow, United Kingdom: Pearson, 2018.

[5] Understanding Cement, "Cement history," [Online]. Available: https://www.understanding-cement.com/history.html. [Accessed 05 02 2024].

[6] C. R. Ragg, "Cement and concrete as an engineering material: An historic appraisal and case study analysis, Engineering Failure Analysis," vol. 40, 2014.

[7] 31 January 2023. [Online]. Available: https://www.statista.com/statistics/1087115/global-cement-production-volume/. [Accessed 16 January 2024].

[8] N. Mahasenan, S. Smith and K. Humphreys, "The Cement Industry and Global Climate Change: Current and Potential Future Cement Industry CO2 Emissions," in *Greenhouse Gas Control Technologies - 6th International Conference*, vol. II, Pergamon, J. Gale, Y. Kaya, 2003.

[9] International Energy Agency (IEA); Cement Sustainability Initiative (CSI), *Cement Technology Roadmap, Low-Carbon Transition in the Cement Industry,* 2009.

[10] M. Enders, R. Teutenberg and P. Sandberg, "Automated calorimetry - the missing link in quality control," 2020.

[11] American Society for Testing and Materials, *Standard Specification for Portland Cement (ASTM C150-07),* 2012.

[12] S. Jianxia, "6.14 - Durability Design of Concrete Hydropower Structures," in *Comprehensive Renewable Energy*, Ali Sayigh, 2012.

[13] Swedish Standards Institute, *Cement - Part 1: Composition, specifications and conformity criteria for common cements (SS-EN 197-1:2011),* 2011.

[14] Q. Song, J. Su, J. Nie, H. Li, Y. Hu, Y. Chen, R. Li and Y. Deng, "The occurrence of MgO and its influence on properties of clinker and cement: A review," *Construction and Building Materials,* vol. 293, no. 123494, 26 July 2021.

[15] D. Herfort and D. E. Macphee, "3 - Components in Portland Cement Clinker and Their Phase Relationships," in *Lea's Chemistry of Cement and Concrete (Fifth Edition)*, Butterworth-Heinemann, 2019.

[16] I. Rikoto and S. Nuhu, "Effect of Free Lime and Lime Saturation Factor on Grindability of Cement Clinker, International Journal of Engineering Research and Reviews," vol. 7, no. 1, 2019.

[17] A. M. Harrisson, "4 - Constitution and Specification of Portland Cement," in *Lea's Chemistry of Cement and Concrete (Fifth Edition)*, Butterworth-Heinemann, 2019.

[18] G. Unland, "Assessment of the grindability of cement clinker, Part 1.," vol. 54, no. 2, 2001.

[19] P. M. Fleiger, R. Reichardt and K. Treiber, "High-Precision Power Measurement for the Grindability Test According to Zeisel.," vol. 35, no. 11, 2012.

[20] The European Cement Association, "About Our Industry - The Manufacturing Process," 2020. [Online]. Available: https://cembureau.eu/about-our-industry/the-manufacturing-process/. [Accessed 16 December 2023].

[21] A. I. Okoji, A. N. Anozie and J. A. Omoleye, "Evaluating the thermodynamic efficiency of the cement grate clinker cooler process using artificial neural networks and ANFIS," vol. 13, no. 5, 2022.

[22] J. W. Bullard, H. M. Jennings, R. A. Livingston, A. Nonat, G. W. Scherer, J. S. Schweitzer, K. L. Scrivener and J. J. Thomas, "Mechanisms of cement hydration," vol. 41, no. 12, 2011.

[23] Ö. Genç and A. Benzer, "Single particle impact breakage characteristics of clinkers related to mineral composition and grindability," vol. 22, no. 13, 2009.

[24] F. G. Ferris, N. Szponar and B. A. Edwards, Groundwater Microbiology, Guelph, Ontario, Canada: Groundwater Project, 2021.

[25] D. P. Bentz, "Three-Dimensional Computer Simulation of Portland Cement Hydration and Microstructure Development," vol. 80, no. 1, 1997.

[26] K. L. Scrivener and A. Nonat, "Hydration of cementitious materials, present and future," vol. 41, no. 7, 2011.

[27] K. L. Scrivener, T. Matschei, F. Georget, P. Juilland and A. K. Mohamed, "Advances in hydration and thermodynamics of cementitious systems," vol. 174, 2023.

[28] E. Gartner, J. Young, D. Damidot and I. Jawed, "Hydration of Portland cement," *Structure and performance of cements,* vol. 2, pp. 57-113, 2002.

[29] T. L. M. &. W. S. D.Sc., "The ice calorimeter of Lavoisier and Laplace and some of its critics," vol. 31, 1974.

[30] L. Wadsö, "Operational issues in isothermal calorimetry," vol. 40, no. 7, 2010.

[31] L. Wadsö, "Applications of an eight-channel isothermal conduction calorimeter for cement hydration studies," no. 5, 2005.

[32] I. Wadsö and R. N. Goldberg, "Standards in Isothermal Microcalorimetry," *International Union of Pure and Applied Chemistry,* vol. 73, no. 10, 2001.

[33] "I-Cal Ultra Isothermal Calorimeter for up to 8 sample cells," 2024. [Online]. Available: https://www.calmetrix.com/i-cal-ultra. [Accessed 02 04 2024].

[34] L. Wadsö, Construction Materials Science, Lund: Building Materials, Lund University, 2017.

[35] "Cement applications, Concepts for Preheaters," 2023. [Online]. Available: https://www.refra.com/en/Preheaters/. [Accessed 03 11 2023].

[36] "Clinker Cooler," 2022. [Online]. Available: https://www.cement-plants.com/clinker-production/clinker-cooler/. [Accessed 03 11 2023].